**Microbial cleavage of C–F bonds in per- and polyfluoroalkyl substances via dehalorespiration**

Yaochun Yu[1], Kunyang Zhang[1], Zhong Li[2], Changxu Ren[3], Jinyong Liu[3], Yujie Men[1,4*]

[1]Department of Civil and Environmental Engineering, University of Illinois at Urbana-Champaign, Urbana, IL, USA.

[2]Metabolomics Center, University of Illinois at Urbana-Champaign, Urbana, IL, USA.

[3]Department of Chemical and Environmental Engineering, University of California, Riverside, Riverside, CA, USA.

[4]Institute for Genomic Biology, University of Illinois at Urbana-Champaign, Urbana, IL, USA.

*Correspondence to: ymen2@illinois.edu

**Abstract**

Regarding the emerging concerns of the widely occurring and environmentally persistent per- and polyfluoroalkyl substances (PFASs), one intriguing and unsolved scientific question for environmental microbiologists, chemists, and engineers is whether microbial reductive defluorination of perfluorinated compounds exists in nature. Due to the strong dissociation energy of carbon–fluorine (C–F) bonds in PFASs, no convincing evidence has ever been reported regarding biological cleavage of C–F bonds from $> C_2$ perfluorinated structures. We, for the first time, show C–F bond cleavage via reductive defluorination by an organohalide-respiring microbial community for two PFASs, perfluoro(4-methylpent-2-enoic acid) and 4,5,5,5-tetrafluoro-4-(trifluoromethyl)-2-pentenoic acid. Comprehensive biotransformation pathways are further elucidated. This study brings valuable fundamental knowledge into microbial dehalorespiration, which opens avenues for the future exploration of PFAS environmental fate and bioremediation strategies.

**One Sentence Summary**

Microbial dehalorespiration of two $C_6$ per- and polyfluorinated structures.

Global concerns on per- and polyfluoroalkyl substances (PFASs) have been rapidly

emerging over the past decade due to their wide applications, environmental persistence,

bioaccumulation, and toxicity to public health and ecosystems *(1)*. PFASs have diverse structures

and ionization forms (anionic, cationic, zwitterionic, and neutral) determined by the chain length

and head groups *(2, 3)*. Thousands of PFAS compounds are on the global market, and a fraction

of them have been identified in representative products such as aqueous film-forming foams

(AFFFs) and commercial goods *(1)*. A number of those identified PFASs, including the legacy

perfluorooctanoic acid (PFOA), perfluorooctanesulfonic acid (PFOS), and the alternative GenX,

have been detected in surface and subsurface drinking water sources, sewage, biosolids, as well

as in humans and animals *(4-8)*. The United States Environmental Protection Agency (USEPA)

has set drinking water health advisory levels for PFOA and PFOS at 70 ng/L *(9)*. Tremendous

efforts have been and are being made to understand the environmental fate and transport of the

structurally diverse PFAS compounds and to develop effective removal strategies.  Due to the

strong Carbon-Fluorine (C–F) bond, the most effective defluorination of PFASs to date is via

physiochemical destruction, including advanced oxidation and reduction, electrochemical,

thermolysis, and plasma-based treatment *(10-14)*. Nonetheless, sporadic reports on microbial

defluorination can be dated back to the 1960s, when aerobic microbial defluorination of

monofluoroacetate via glycolate-forming, C–F bond hydrolysis was observed, and the

corresponding hydrolytic dehalogenase was identified *(15)*. Stepwise reductive defluorination of

trifluoroacetate (TFA, $CF_3COOH$) to acetate via di- and monofluoroacetate in a methanogenic

microbial community was documented two decades ago *(16, 17)*. However, no follow-up study

investigated the responsible microorganisms, enzymes, or the defluorination mechanisms. In

addition to fluoroacetates, monofluoroaromatics such as 2- and 4-fluorobenzoate have been

24  observed to undergo biodefluorination under denitrifying conditions by enoyl-CoA

25  hydratases/hydrolases and an ATP-dependent class I BzCoA reductase, respectively *(18, 19)*.

26  However, regarding typical PFASs with carbon chains longer than TFA, microbial defluorination

27  has only been observed for telomeric structures (with $-CH_2$ groups on the carbon backbone) and

28  their polymers rather than perfluorinated ones *(20-24)*. Fluorotelomer alcohols (FTOHs),

29  carboxylic acids (FTCAs) and sulfonic acids (FTSAs) are all found to be partially

30  biotransformed into perfluoroalkyl acids (PFAAs) under both aerobic and anaerobic conditions,

31  suggesting potential sources of PFAAs *(25, 26)*. The responsible microorganisms/enzymes and

32  the underlying mechanisms are still unknown.

33      The question that has been scientifically and practically intriguing but not well addressed

34  is this: can microbes break down perfluorinated compounds longer than TFA or not at all?

35  Although reductive defluorination of perfluorinated compounds is biologically feasible

36  according to the thermodynamic calculations *(27)*, to our best knowledge, there is no convincing

37  evidence reported for microbial cleavage of the C–F bond in non-TFA perfluorinated

38  compounds, in terms of both fluoride ion release and the corresponding transformation product

39  formation *(26)*. Inspired by the very recent studies, in which abiotic reductive defluorination of

40  branched PFASs slowly occurred in a vitamin $B_{12}$-Ti$^{III}$ catalytic system at room temperature *(10,*

41  *28)*, we hypothesized that biological reductive defluorination of branched PFASs could be

42  carried out by organohalide-respiring microorganisms that possess $B_{12}$-dependent reductive

43  dehalogenases *(29, 30)*. In this study, we fill the knowledge gap by demonstrating the occurrence

44  of microbial reductive defluorination of branched, unsaturated per- and polyfluoroalkyl

45  structures and identifying the corresponding defluorination pathways. These groundbreaking

46  findings open new avenues of investigating and developing PFAS biodegradation technologies to

remediate contaminated subsurface environments. The structural specificity of microbial

reductive defluorination can also guide the design of more environmentally friendly PFAS

structures.

**Reductive defluorination of select PFASs by a dechlorinating enrichment.** The

dehalorespiration of PFASs was investigated in the subsequent transfers (10%, v/v) of a well-

studied and commercially available dechlorinating enrichment culture KB-1® (SiREM, Ontario,

Canada). Five PFAS structures were tested: three perfluorinated ones, i.e., PFOA (linear,

saturated, long-chain, $C_8$), perfluoro-3,7-dimethyloctanoic acid (PFdiMeOA; branched,

saturated, long-chain, $C_{10}$), and perfluoro(4-methylpent-2-enoic acid) (PFMeUPA; branched,

unsaturated, short-chain, $C_6$), as well as two polyfluorinated ones structurally similar to

PFMeUPA: 4,5,5,5-tetrafluoro-4-(trifluoromethyl)-2-pentenoic acid (FTMeUPA; branched,

unsaturated, short-chain, $C_6$) and 4,5,5,5tetrafluoro-4-(trifluoromethyl) pentanoic acid (FTMePA;

branched, saturated, short-chain, $C_6$) (Table S1). Given the difficulty to break C–F bonds in

PFASs, it is extraordinarily fascinating to obtain strong evidence in terms of the parent

compound removal and F⁻ release for microbial reductive defluorination of the two unsaturated

$C_6$ PFASs, particularly the perfluorinated PFMeUPA (Fig. 1A–D). Both of them can serve as the

sole electron acceptor with not only organic carbons like lactate but also hydrogen (Fig. S1) as

the primary electron donor, which is evident for reductive defluorination. The defluorination was

much slower compared to the dechlorination of trichloroethene (TCE) by the same culture (Fig.

S2). It took ~ 130 days for the complete removal of 75 µM PFMeUPA, while only ~ 70 days for

the same molar concentration of polyfluorinated FTMeUPA. It is not surprising to see faster

microbial anaerobic degradation of the telomeric PFASs *(20, 26)*, which are more readily

degradable than perfluorinated ones due to the presence of Carbon-Hydrogen (C–H) bonds.

Moreover, the lack of observed microbial defluorination for the saturated FTMePA (Fig. S3A) suggests that the presence of the double bond (C=C) facilitated the microbial defluorination of PFMeUPA and FTMeUPA. For the tested long-chain PFASs, i.e., PFOA and PFdiMeOA, no microbial defluorination was observed (Fig. S3B–C). The recalcitrance of PFOA to microbial defluorination is consistent with the findings from other studies *(26, 31)*. The branched structure in PFdiMeOA seems not to enhance its biodegradability by the investigated culture.
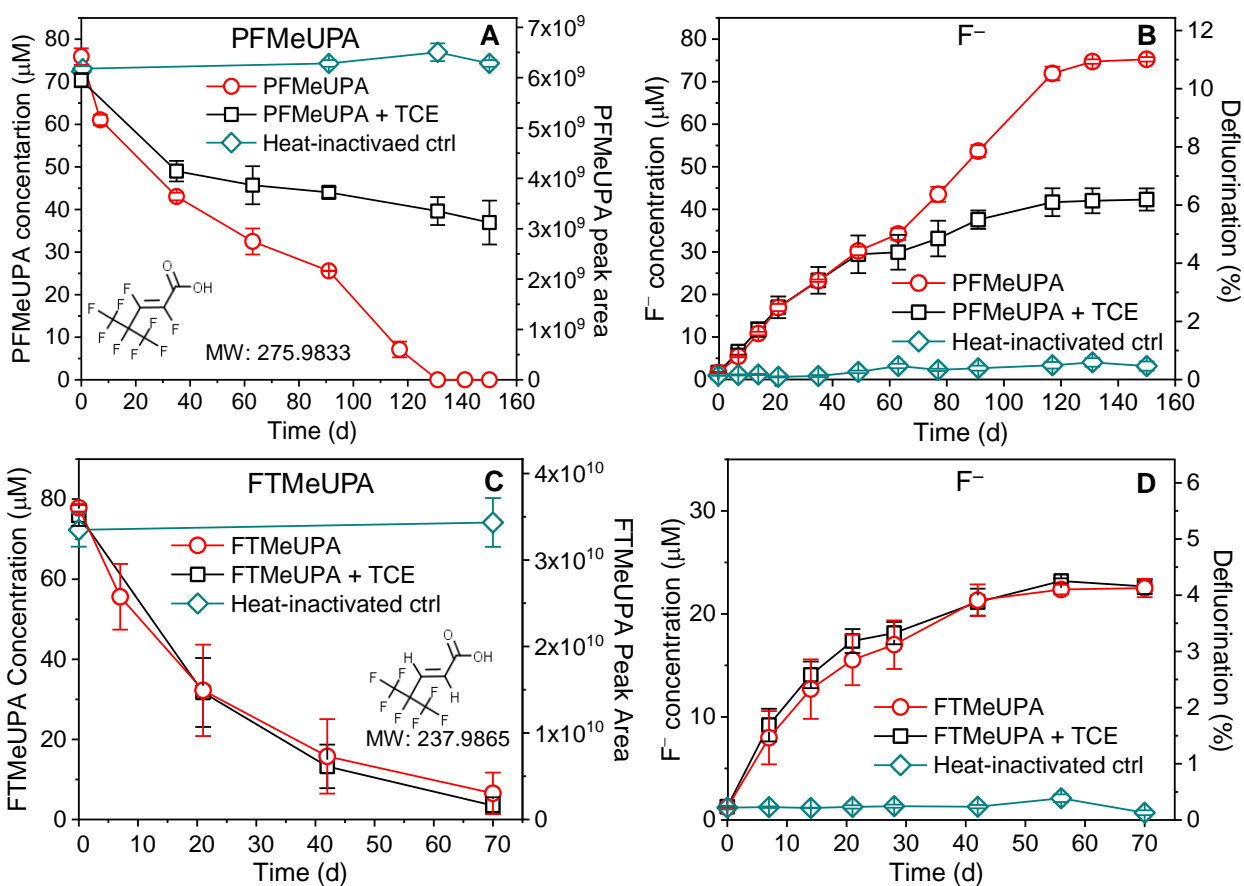


**Fig. 1**. Decay and fluoride ion release of PFMeUPA (A & B) and FTMeUPA (C & D) in the dehalorespiring microbial community.

**Transformation product (TP) analysis reveals the C–F bond cleavage positions and the biodegradation pathways of PFMeUPA and FTMeUPA.** According to the suspect and non-target TP screening criteria (see Materials and Methods in the SI), twelve TPs of PFMeUPA and six TPs of FTMeUPA were identified (Table S1), indicating that the two PFASs underwent multiple biotransformation pathways besides reductive defluorination. For TPs with the reference compounds available, their structures were confirmed by matched tandem mass spectrometry ($MS^2$) fragments to the $MS^2$ spectra of the authentic standard. For TPs without available standards, their structures were inferred according to the $MS^2$ spectra and the similarity to the ones predicted by a web-based competitive fragment modeling tool CFM-ID 2.0 (see Materials and Methods in the SI) (Fig. S4–S22, Table S1) *(32)*. Confirmed and plausible structures of TPs are given in Fig. 3 & 4. Only TPs with authentic standards were quantified. For the other TPs, peak areas were used to interpret their formation trend over a time course. We are aware of the difference in MS ionization efficiency among different PFASs and their TPs. As such differences among the available reference compounds were less than 10-fold (Table S2), the same ionization efficiency was used for a rough estimation of the relative abundance among TPs with more than one order of magnitude difference in peak areas.

For PFMeUPA, TP256 (–F+H from PFMeUPA) is the corresponding TP from the first step of reductive defluorination (Fig. 2A and Reaction 1 in Fig. 3). TP256 has an $MS^2$ fragment of $C_3F_7^-$ (Fig. S5), indicating that the first C−F bond cleavage was at the $sp^2$ C−F bond on one of the unsaturated carbons in PFMeUPA. Similarly, the first C−F bond cleaved during the $B_{12}$-catalyzed abiotic defluorination of 2,3,3,3-tetrafluoropropene was also at the $sp^2$ C−F bond on the unsaturated carbon *(33)*. Additionally, it is worth noting that although the tertiary $sp^3$ C−F bond in PFMeUPA has the lowest bond dissociation energy (BDE) (Fig. 3), the formation of

TP256 indicates that the $sp^2$ C−F bonds are more microbially active. Due to the very similar BDE

values for the two $sp^2$ C−F bonds in PFMeUPA (Fig. 3), it is not clear which of the two C−F

bonds first underwent the F→H exchange. The $MS^2$ profile of TP256 does not provide any

clearer evidence, either. The microbial reductive defluorination of PFMeUPA is much slower

and to a lower defluorination extent than the chemical reductive defluorination of PFMeUPA

with a $B_{12}$-$Ti^{III}$ catalytic system *(10)*. This could be due to different defluorination mechanisms

between biological and abiotic systems or to the low enzyme abundance and activity.
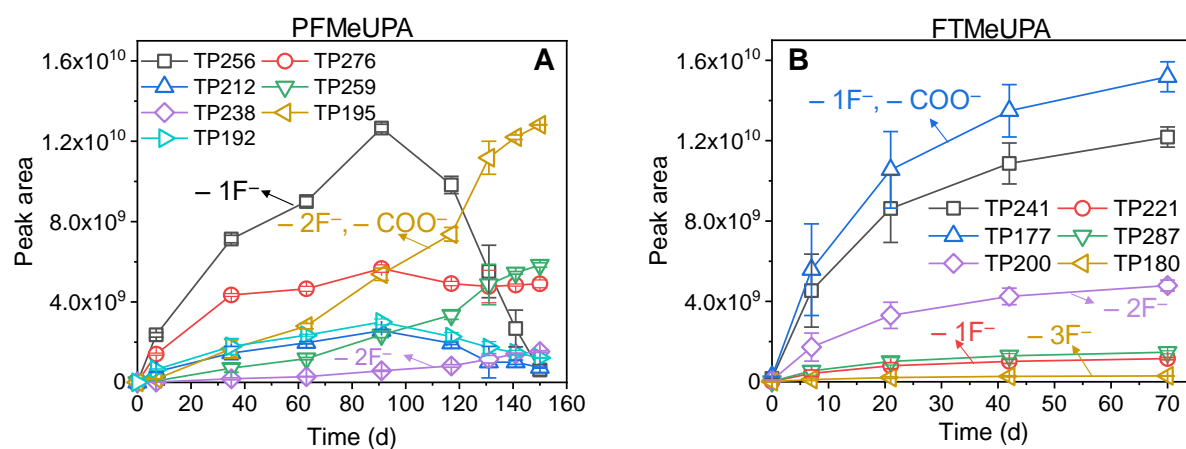


**Fig. 2**. TP formation during the biotransformation of PFMeUPA (A) and FTMeUPA (B) by the

dehalorespiring community (arrows indicate TPs formed from defluorination reactions).


As PFMeUPA was being continuously transformed, TP256 was accumulated during the

first 90 days, followed by a significant decrease, suggesting secondary biotransformation (Fig.

2A). The secondary biotransformation includes multiple routes. One major pathway was the

formation of TP212 from decarboxylation of TP256 (Reaction 3 in Fig. 3). TP212 was only

slightly accumulated, and further transformed into several downstream defluorination products

(i.e., TP195, TP192, TP174, and TP154). Unlike TP256 and TP212, the second C−F bond

cleavage products, TP195 and TP192, did not show the $MS^2$ fragment of $C_3F_7^-$ (Table S1 and

Fig. S12). This suggests that rather than the remaining $sp^2$ C−F bond on the unsaturated carbon,

the second defluorination occurred within the –$C_3F_7$ group. TP195 was likely from the reductive

defluorination of TP212 (Reactions 6 in Fig. 3), which was highly accumulated after the 150-day

incubation period (Fig. 2A). The $sp^3$ C−F bond in the –$C_3F_7$ group has the lowest BDE, thus

more likely to be cleaved. Furthermore, the behavior of TP195 on the LC-HRMS/MS was

different from the authentic standard of the $sp^2$ C−F cleavage product (3-(trifluoromethyl)-

3,4,4,4-tetrafluorobutene-1) (Table S1), indicating a different structure of TP195. TP192, as well

as the third and fourth C−F bond cleavage products (TP174 and TP154) were at relatively low

abundances (Fig. 2A & S23). Due to their unclear structures, the formation routes of these three

TPs are ambiguous and hypothetical (Reactions 7, 13 − 16 in Fig. 3).
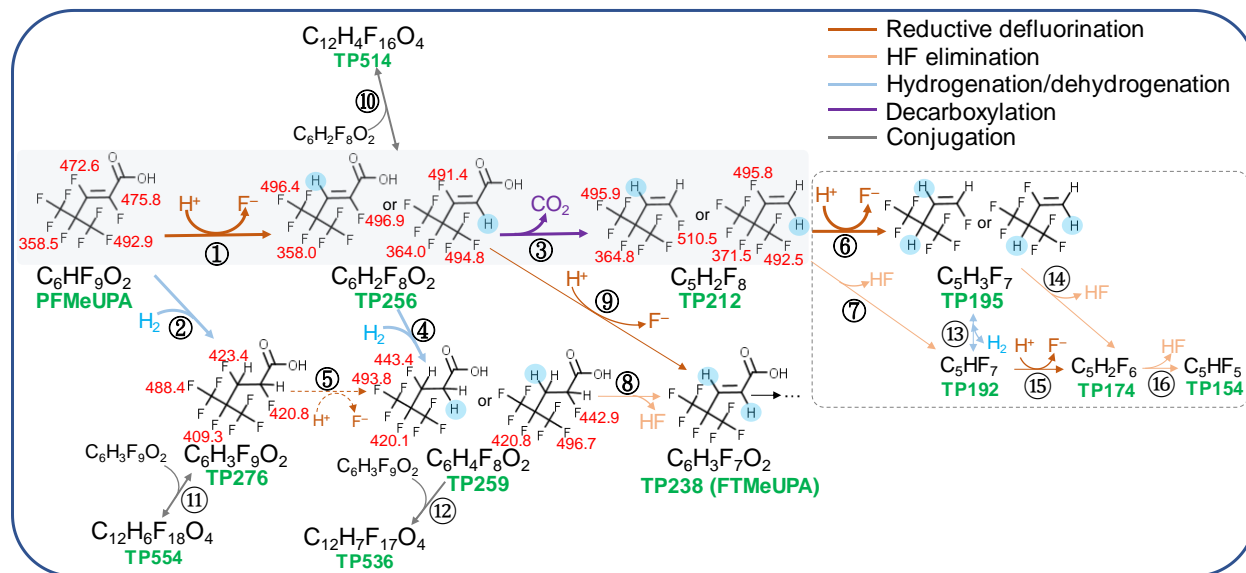


**Fig. 3.** Proposed biotransformation pathways of PFMeUPA in the dehalorespiring community

(defluorination positions are shaded in blue; dashed arrows for Reaction 6 represent reductive

defluorination of a saturated perfluorinated carboxylic acid; the red number next to a C−F bond

is the calculated bond dissociation energy in kJ/mol); gray box: the major biotransformation

pathway of PFMeUPA; dashed box: tentative downstream pathways.

Besides the major reductive defluorination route, PFMeUPA also underwent a branched

route of bioreduction (a.k.a. hydrogenation) forming a saturated fluorinated carboxylic acid

TP276 (Fig. 2 and Reaction 2 in Fig. 3). Similarly, another saturated TP (TP259) was formed,

likely from the partial hydrogenation of TP256 (Fig. 2 and Reaction 4 in Fig. 3). The

hydrogenation of unsaturated polyfluorinated substances has also been observed in both aerobic

and anaerobic sludges *(20, 22)*. The hydrogenation of α, β-unsaturated carboxylic anions forming

the corresponding saturated carboxylic acids can be catalyzed by enoate reductases with

nicotinamide adenine dinucleotide (NADH) as the cofactor from anaerobic microorganisms such

as *Clostridium kluyveri (34)*. Flavin-based ene-reductases from the "Old Yellow Enzyme" family

possessed by a variety of microorganisms may also carry out the reduction of activated alkenes

with carboxylic acid as the electron withdrawing group (EWG) when there is an additional EWG

such as a halogen *(35)*. It is still unclear whether such hydrogenation reactions are energy-

yielding and metabolically essential to sustain the growth of the carrying microorganisms *(34)*.

Besides the hydrogenation pathway, TP259 could also be formed from another route via

microbial defluorination of TP276 (Reaction 5 in Fig. 3). The BDE values of the two C−F bonds

on Carbon 2 and Carbon 3 in TP276 are similar to the BDE values of the other C−F bonds in

TP276 (Fig. 3), as well as the C−F BDE values in the structurally similar saturated FTMePA

(Fig. 4). As FTMePA did not undergo any defluorination reaction (Fig. S3A), the microbial

reductive defluorination of TP276 is thus less likely.

Another secondary TP of PFMeUPA is TP238, which was confirmed to be FTMeUPA

(Fig. S13). TP238 was possibly formed directly from the reductive defluorination of TP256

(Reaction 9 in Fig. 3) or from hydrogenation of TP256 followed by HF elimination (Reactions 4

& 8 in Fig. 3). Both pathways have been previously shown in the biotransformation of 8:2 and

6:2 fluorotelomeric alcohols/acids in anaerobic sludges *(22, 24)*. The HF elimination reactions

may occur both abiotically and biologically (mediated by enzymes like acyl-CoA

dehydrogenases) *(36)*. The maximum concentration of TP238 (i.e., FTMeUPA) in the

PFMeUPA biotransformation samples was less than 3 μM (< 4% of the added PFMeUPA).

Given that FTMeUPA can be biotransformed by the same community (Fig. 1C), the low level of

FTMeUPA (TP238) during PFMeUPA biotransformation could be attributed to a secondary

degradation. To elucidate this, we analyzed the TPs during FTMeUPA biotransformation and

their formation during PFMeUPA biotransformation.
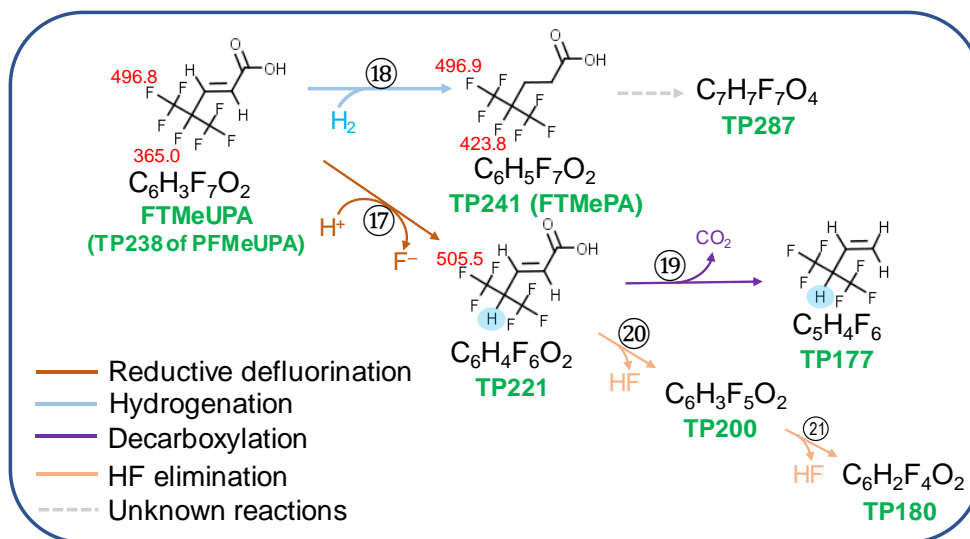


**Fig. 4**. Proposed biotransformation pathways of FTMeUPA in the dehalorespiring community

(defluorination positions are shaded in blue; dashed arrows represent unknown reactions; the red

number next to a C−F bond is the calculated bond dissociation energy in kJ/mol).

Like PFMeUPA, FTMeUPA underwent two major primary biotransformation pathways,

reductive defluorination at the $sp^3$ C−F bond (with the lowest BDE) forming TP221) and

hydrogenation forming TP241 (confirmed to be FTMePA) (Fig. 4). TP241 was accumulated

along with incubation, consistent with the recalcitrance of FTMePA to microbial degradation

179 (Fig. 2B & S3A). TP221 was in relatively low abundance likely due to the rapid conversion to

180 secondary TPs via decarboxylation and/or HF elimination (Fig. 2B & 4). Among all FTMeUPA

181 TPs, only TP241 was slightly detected in the PFMeUPA biotransformation samples, indicating

182 that the FTMeUPA formation (Reactions 8 & 9 in Fig. 3) was only a minor pathway of

183 PFMeUPA biotransformation.

184 Another minor route during PFMeUPA biotransformation is the conjugation of TP256

185 and TP276, forming their dimers, i.e., TP514 and TP554, respectively (Reactions 10 and 11 in

186 Fig. 3). TP536 from the conjugation of TP276 and TP259 was also formed (Reaction 12 in Fig.

187 3). TP514 significantly decreased after 90 days (Fig. S23), likely being back-transformed to

188 TP256 while TP256 was being further converted to the downstream TPs (Fig. 2A).

189 Collectively, PFMeUPA first underwent both reductive defluorination (the first C−F

190 bond cleavage) and hydrogenation pathways, which should result in a total defluorination less

191 than what would have been expected if all PFMeUPA was subject to the first C−F bond cleavage

192 (11%). The actual observed ~11% total defluorination is thus attributed to further defluorination

193 (more than one C−F bond cleavage). FTMeUPA underwent the same major pathways as

194 PFMeUPA. The large formation of the hydrogenation TP (TP241) in addition to the

195 defluorination TPs agrees with the 4% total defluorination of FTMeUPA, which corresponds to

196 less than one fluorine released per molecule (the total theoretical defluorination is 14% if all

197 FTMeUPA underwent the first C−F bond cleavage). Notably, Reactions 1 & 6 in Fig. 3 and

198 Reaction 16 in Fig. 4 are novel microbial reductive defluorination reactions. Unveiling the

199 microbial capabilities of breaking the "hardest-ever" carbon−halogen bond via reductive

200 dehalogenation and elucidating the overall pathways are of great scientific significance and

technological importance for the understanding of PFAS biodegradability and the development of treatment strategies.

***Dehalococcoides* spp. were not responsible for the defluorination, while *Dehalobacter* spp. were likely involved in downstream biotransformation pathways**. The dominant dechlorinator in the investigated KB-1 culture is *Dehalococcoides* spp. *(37)*. The versatility of $B_{12}$-dependent reductive dehalogenases of *Dehalococcoides* spp. in metabolizing various organohalides makes them the most promising candidates capable of microbial reductive defluorination of the two PFASs *(38)*. Thus, we first looked at the growth and activities of *Dehalococcoides* spp. in the PFMeUPA/FTMeUPA-fed culture. Unexpectedly, no *Dehalococcoides* activity or growth was observed during the incubation period when PFMeUPA/FTMeUPA was provided as the sole electron acceptor, in terms of the 16S rRNA gene abundance and its transcription level, as well as the transcription levels of 14 identified reductive dehalogenase (RDase) genes in the same community *(39)* (Fig. 5A & B, Fig. S24A & B, and Fig. S25). The lack of growth of *Dehalococcoides* was also reflected by the decrease in the total bacterial growth (Fig. 5C). In comparison, cultures with TCE addition exhibited active growth of *Dehalococcoides* (Fig. 5A & B). Theoretically, the energy generated from the added PFMeUPA/FTMeUPA (75 μM) can sustain the growth of *Dehalococcoides* via reductive dehalogenation if it occurs. Therefore, the dominant chloroethene-respiring *Dehalococcoides* spp. in the community were not responsible for the reductive defluorination of PFMeUPA/FTMeUPA. Corroboratively, the two isolated *Dehalococcoides* strains, *D. mccartyi* FL2 and BAV1, were not able to cleave $F^-$ from PFMeUPA while the cells exhibited dechlorination activities (Fig. S26).

Instead of contributing to defluorination, the presence of TCE and/or dechlorination activity of *Dehalococcoides* inhibited the defluorination of PFMeUPA after 30 – 50 days (Fig. 1A & B), while no inhibition for FTMeUPA during the entire incubation period (Fig. 1C & D). The inhibition was less likely caused by substrate competition because the substrate lactate was added intermittently in excess throughout the entire incubation period. Thus, we inferred that different microbial groups were involved in the defluorination of the two compounds, and TCE specifically inhibited the PFMeUPA-defluorinating species.
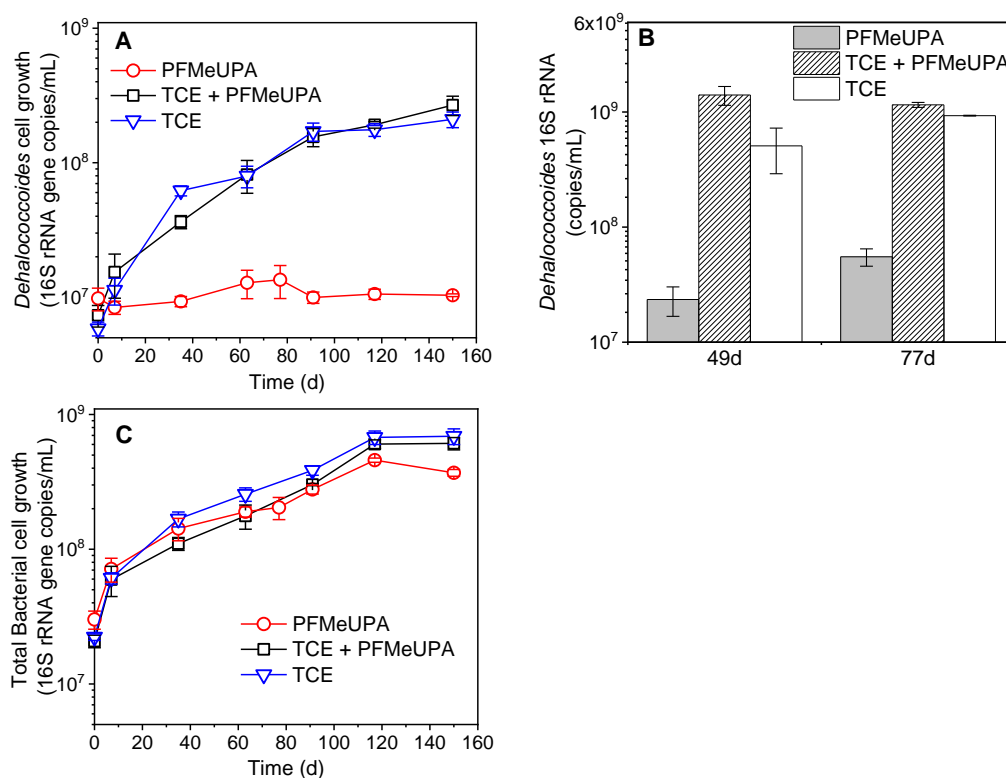


**Fig. 5**. The growth of *Dehalococcoides* spp. as the 16S rRNA gene copy numbers (A), *Dehalococcoides* spp. activities as the 16S rRNA copy numbers (B), and the total bacterial growth as the total 16S rRNA gene copy numbers (C).

We then looked at the growth of another two dechlorinators in this community: the

second dominant TCE-dechlorinating species *Geobacter* spp. in addition to *Dehalococcoides*

*(37)* and the recently identified trichlorobenzene (TCB)-dechlorinating species *Dehalobacter* spp

*(40)*. Again, *Geobacter* spp. showed no growth in the PFMeUPA-fed culture, hence were not

responsible for the reductive defluorination. Nevertheless, we observed significantly higher

growth and activities (in terms of cell densities and 16S rRNA levels) of *Dehalobacter* in the

PFMeUPA/FTMeUPA-fed culture compared to the TCE-fed ones (Fig. 6 and Fig. S24C). One

should note that the initial abundance of *Dehalobacter* in the seed culture fed with TCE was

extremely low ($< 10^3$/mL). Such low *Dehalobacter* abundance was consistent with what was

observed in the TCE-fed subcultures of the same microbial community *(40)*. Several

*Dehalobacter* strains have been demonstrated to biodegrade chlorinated compounds such as

TCE, trichloroethane (TCA), and TCB *(40-42)*. A similar emergence of *Dehalobacter* population

with a significant decrease of *Dehalococcoides* population was observed when the terminal

electron acceptor was switched from TCE to 1,2,4-TCB *(41)*. The abilities of *Dehalobacter* spp.

to utilize diverse chlorinated compounds to alleviate substrate competition with other

dehalorespiring microorganisms make them likely involved in the defluorination of PFMeUPA

and FTMeUPA. Thus, we further examined the defluorination capabilities of the pure culture of

*Dehalobacter restrictus* strain PER-K23, the closest one to *Dehalobacter* spp. in the community

*(40)*, but we did not detect any F⁻ release from PFMeUPA and FTMeUPA (Fig. S27A & B).

Nonetheless, one may still not exclude the possibility that the actual *Dehalobacter* spp. in the

community were able to carry out the reductive defluorination of PFMeUPA or the

biotransformation intermediates of PFMeUPA, such as the first C−F bond cleavage product

TP256. Because there was not a sufficient amount of authentic or isolated TP256 available, the

259     actual role of *Dehalobacter* spp. on the PFMeUPA and FTMeUPA

260     defluorination/biotransformation remains elusive.
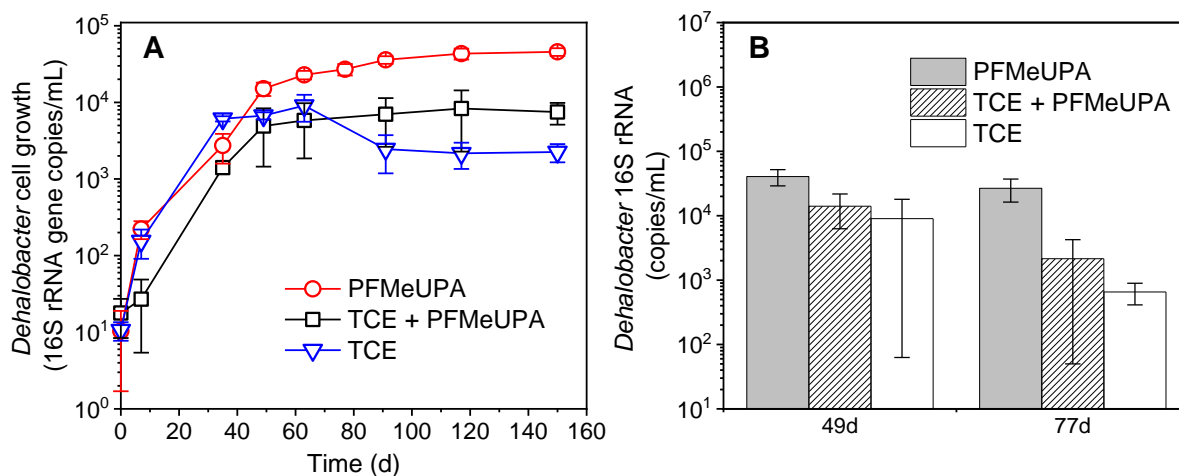


261

262     **Fig. 6**. The growth of *Dehalobacter* spp. as its 16S rRNA gene copy numbers (A), *Dehalobacter*

263     spp. activities as the 16S rRNA copy numbers (B).

264

265             According to this study, unsaturated perfluorinated compounds seem to be more

266     bioavailable, and the first C−F bond cleavage at the *sp2* position is crucial for the following

267     stepwise defluorination to occur. As the dominant dechlorinating species in the community were

268     not responsible for the PFMeUPA/FTMeUPA defluorination, the actual defluorinating

269     microorganisms are likely in low abundance in this community, rendering the slow activities for

270     the two compounds. The low abundance might also cause no defluorination for the other tested

271     long-chain and saturated PFASs, because the defluorination can be kinetically limited for those

272     more recalcitrant structures. Thus, higher activities and perhaps a wider PFAS substrate range is

273     expected for enriched, isolated, and acclimated PFMeUPA/FTMeUPA-defluorinating

274     microorganisms. While the enrichment, identification, and isolation are still ongoing due to the

275     slow growth of the defluorinating culture, considering the commercial use and environmental

276   occurrence of unsaturated PFASs *(43, 44)*, the present findings already open various

277   opportunities for PFAS management and treatment in the future. These include finding

278   alternative PFASs with more readily biodegradable structures, assessing the environmental fate

279   of branched and unsaturated PFASs, and developing biotechnologies and treatment train systems

280   for PFAS removal and destruction.

281

282   **REFERENCES AND NOTES**

283   (1)     Wang, Z.; DeWitt, J. C.; Higgins, C. P.; Cousins, I. T. A never-ending story of per- and

284   polyfluoroalkyl substances (PFASs)? *Environ. Sci. Technol.* **51**, 2508-2518 (2017).

285   (2)     D'Agostino, L. A.; Mabury, S. A. Identification of novel fluorinated surfactants in

286   aqueous film forming foams and commercial surfactant concentrates. *Environ. Sci. Technol.* **48**,

287   121-129 (2014).

288   (3)     Xiao, F.; Golovko, S. A.; Golovko, M. Y. Identification of novel non-ionic, cationic,

289   zwitterionic, and anionic polyfluoroalkyl substances using UPLC-TOF-MS(E) high-resolution

290   parent ion search. *Anal. Chim. Acta.* **988**, 41-49 (2017).

291   (4)     Xiao, F. Emerging poly- and perfluoroalkyl substances in the aquatic environment: a

292   review of current literature. *Water Res.* **124**, 482-495 (2017).

293   (5)     Sun, M.; Arevalo, E.; Strynar, M.; Lindstrom, A.; Richardson, M.; Kearns, B.; Pickett,

294   A.; Smith, C.; Knappe, D. R. U. Legacy and emerging perfluoroalkyl substances are important

295   drinking water contaminants in the Cape Fear River watershed of North Carolina. *Environ. Sci.*

296   *Technol. Lett.* **3**, 415-419 (2016).

297   (6)     Boulanger, B.; Vargo, J. D.; Schnoor, J. L.; Hornbuckle, K. C. Evaluation of

298   perfluorooctane surfactants in a wastewater treatment system and in a commercial surface

299   protection product. *Environ. Sci. Technol.* **39**, 5524-5530 (2005).

300   (7)     Lindstrom, A. B.; Strynar, M. J.; Delinsky, A. D.; Nakayama, S. F.; McMillan, L.;

301   Libelo, E. L.; Neill, M.; Thomas, L. Application of WWTP biosolids and resulting perfluorinated

302   compound contamination of surface and well water in Decatur, Alabama, USA. *Environ. Sci.*

303   *Technol.* **45**, 8015-8021 (2011).

304   (8)     Sepulvado, J. G.; Blaine, A. C.; Hundal, L. S.; Higgins, C. P. Occurrence and fate of

305   perfluorochemicals in soil following the land application of municipal biosolids. *Environ. Sci.*

306   *Technol.* **45**, 8106-8112 (2011).

307   (9)     U.S. Environmental Protection Agency, (EPA). "PFOA & PFOS drinking water health

308   advisories"; (Publication 800-F-16-003, EPA, 2016, www.epa.gov/sites/production/files/2016-

309   06/documents/drinkingwaterhealthadvisories_pfoa_pfos_updated_5.31.16.pdf).

310   (10)     Liu, J.; Van Hoomissen, D. J.; Liu, T.; Maizel, A.; Huo, X.; Fernández, S. R.; Ren, C.;

311   Xiao, X.; Fang, Y.; Schaefer, C. E.; Higgins, C. P.; Vyas, S.; Strathmann, T. J. Reductive

312   defluorination of branched per- and polyfluoroalkyl substances with cobalt complex catalysts.

313   *Environ. Sci. Technol. Lett.* **5**, 289-294 (2018).

314   (11)     Schaefer, C. E.; Choyke, S.; Ferguson, P. L.; Andaya, C.; Burant, A.; Maizel, A.;

315   Strathmann, T. J.; Higgins, C. P. Electrochemical transformations of perfluoroalkyl acid (PFAA)

316   precursors and PFAAs in groundwater impacted with aqueous film forming foams. *Environ. Sci.*

317   *Technol.* **52**, 10689-10697 (2018).

318    (12)    Vecitis, C. D.; Park, H.; Cheng, J.; Mader, B. T.; Hoffmann, M. R. Treatment

319    technologies for aqueous perfluorooctanesulfonate (PFOS) and perfluorooctanoate (PFOA).

320    *Front. Environ. Sci. Eng.* **3**, 129-151 (2009).

321    (13)    Stratton, G. R.; Dai, F.; Bellona, C. L.; Holsen, T. M.; Dickenson, E. R. V.; Mededovic

322    Thagard, S. Plasma-based water treatment: Efficient transformation of perfluoroalkyl substances

323    in prepared solutions and contaminated groundwater. *Environ. Sci. Technol.* **51**, 1643-1648

324    (2017).

325    (14)    Bentel, M. J.; Yu, Y. C.; Xu, L. H.; Li, Z.; Wong, B. M.; Men, Y. J.; Liu, J. Y.

326    Defluorination of per- and polyfluoroalkyl substances (PFASs) with hydrated electrons:

327    structural dependence and implications to PFAS remediation and management. *Environ. Sci.*

328    *Technol.* **53**, 3718-3728 (2019).

329    (15)    Goldman, P. The enzymatic cleavage of the carbon-fluorine bond in fluoroacetate. *J.*

330    *Biol. Chem.* **240**, 3434-3438 (1965).

331    (16)    Visscher, P. T.; Culbertson, C. W.; Oremland, R. S. Degradation of trifluoroacetate in

332    oxic and anoxic sediments. *Nature* **369**, 729-731 (1994).

333    (17)    Kim, B. R.; Suidan, M. T.; Wallington, T. J.; Du, X. Biodegradability of trifluoroacetic

334    acid. *Environ. Eng. Sci.* **17**, 337-342 (2000).

335    (18)    Tiedt, O.; Mergelsberg, M.; Eisenreich, W.; Boll, M. Promiscuous defluorinating enoyl-

336    CoA hydratases/hydrolases allow for complete anaerobic degradation of 2-fluorobenzoate.

337    *Front. Microbiol.* **8**, 2579 (2017).

338    (19)    Tiedt, O.; Mergelsberg, M.; Boll, K.; Muller, M.; Adrian, L.; Jehmlich, N.; von Bergen,

339    M.; Boll, M. ATP-dependent C-F bond cleavage allows the complete degradation of 4-

340    fluoroaromatics without oxygen. *Mbio* **7**, e00990-16 (2016).

341     (20)    Wang, N.; Szostek, B.; Buck, R. C.; Folsom, P. W.; Sulecki, L. M.; Capka, V.; Berti, W.

342     R.; Gannon, J. T. Fluorotelomer alcohol biodegradation-direct evidence that perfluorinated

343     carbon chains breakdown. *Environ. Sci. Technol.* **39**, 7516-7528 (2005).

344     (21)    Shaw, D. M. J.; Munoz, G.; Bottos, E. M.; Duy, S. V.; Sauve, S.; Liu, J.; Van Hamme, J.

345     D. Degradation and defluorination of 6:2 fluorotelomer sulfonamidoalkyl betaine and 6:2

346     fluorotelomer sulfonate by *Gordonia* sp. strain NB4-1Y under sulfur-limiting conditions. *Sci.*

347     *Total. Environ.* **647**, 690-698 (2019).

348     (22)    Zhang, S.; Szostek, B.; McCausland, P. K.; Wolstenholme, B. W.; Lu, X.; Wang, N.;

349     Buck, R. C. 6:2 and 8:2 fluorotelomer alcohol anaerobic biotransformation in digester sludge

350     from a WWTP under methanogenic conditions. *Environ. Sci. Technol.* **47**, 4227-4235 (2013).

351     (23)    Lee, H.; D'eon, J.; Mabury, S. A. Biodegradation of polyfluoroalkyl phosphates as a

352     source of perfluorinated acids to the environment. *Environ. Sci. Technol.* **44**, 3305-3310 (2010).

353     (24)    Li, F.; Su, Q. F.; Zhou, Z. M.; Liao, X. B.; Zou, J.; Yuan, B. L.; Sun, W. J. Anaerobic

354     biodegradation of 8:2 fluorotelomer alcohol in anaerobic activated sludge: metabolic products

355     and pathways. *Chemosphere* **200**, 124-132 (2018).

356     (25)    Butt, C. M.; Muir, D. C.; Mabury, S. A. Biotransformation pathways of fluorotelomer-

357     based polyfluoroalkyl substances: a review. *Environ. Toxicol. Chem.* **33**, 243-267 (2014).

358     (26)    Liu, J.; Mejia Avendano, S. Microbial degradation of polyfluoroalkyl chemicals in the

359     environment: a review. *Environ. Int.* **61**, 98-114 (2013).

360     (27)    Parsons, J. R.; Sáez, M.; Dolfing, J.; de Voogt, P. "Biodegradation of perfluorinated

361     compounds" in *Reviews of environmental contamination and toxicology*, Whitacre, D. M., Ed.

362     (Springer US, 2008); vol. 196 pp. 53-71.

(28)     Park, S.; de Perre, C.; Lee, L. S. Alternate reductants with VB$_{12}$ to transform C8 and C6 perfluoroalkyl sulfonates: limitations and insights into isomer specific transformation rates, products and pathways. *Environ. Sci. Technol.* **51**, 13869-13877 (2017).

(29)     Fincker, M.; Spormann, A. M. Biochemistry of catabolic reductive dehalogenation. *Annu. Rev. Biochem.* **86**, 357-386 (2017).

(30)     Schubert, T.; Adrian, L.; Sawers, R. G.; Diekert, G. Organohalide respiratory chains: composition, topology and key enzymes. *FEMS Microbiol. Ecol.* **94**, (2018).

(31)     Ochoa-Herrera, V.; Field, J. A.; Luna-Velasco, A.; Sierra-Alvarez, R. Microbial toxicity and biodegradability of perfluorooctane sulfonate (PFOS) and shorter chain perfluoroalkyl and polyfluoroalkyl substances (PFASs). *Environ. Sci. Process. Impacts* **18**, 1236-1246 (2016).

(32)     Pon, A.; Wishart, D.; Wilson, M.; Greiner, R.; Allen, F. CFM-ID: a web server for annotation, spectrum prediction and metabolite identification from tandem mass spectra. *Nucleic Acids Res.* **42**, W94-W99 (2014).

(33)     Im, J.; Walshe-Langford, G. E.; Moon, J. W.; Löffler, F. E. Environmental fate of the next generation refrigerant 2,3,3,3-tetrafluoropropene (HFO-1234yf). *Environ. Sci. Technol.* **48**, 13181-13187 (2014).

(34)     Tischer, W.; Bader, J.; Simon, H. Purification and some properties of a hitherto-unknown enzyme reducing the carbon-carbon double bond of α,β-unsaturated carboxylate anions. *Eur. J. Biochem.* **97**, 103-112 (1979).

(35)     Winkler, C. K.; Tasnádi, G.; Clay, D.; Hall, M.; Faber, K. Asymmetric bioreduction of activated alkenes to industrially relevant optically active compounds. *J. Biotechnol.* **162**, 381-389 (2012).

385     (36)     Dinglasan, M. J. A.; Ye, Y.; Edwards, E. A.; Mabury, S. A. Fluorotelomer alcohol

386     biodegradation yields poly- and perfluorinated acids. *Environ. Sci. Technol.* **38**, 2857-2864

387     (2004).

388     (37)     Duhamel, M.; Edwards, E. A. Microbial composition of chlorinated ethene-degrading

389     cultures dominated by *Dehalococcoides*. *FEMS Microbiol. Ecol.* **58**, 538-549 (2006).

390     (38)     Löffler, F. E.; Yan, J.; Ritalahti, K. M.; Adrian, L.; Edwards, E. A.; Konstantinidis, K. T.;

391     Müller, J. A.; Fullerton, H.; Zinder, S. H.; Spormann, A. M. *Dehalococcoides mccartyi* gen.

392     nov., sp. nov., obligately organohalide-respiring anaerobic bacteria relevant to halogen cycling

393     and bioremediation, belong to a novel bacterial class, *Dehalococcoidia* classis nov., order

394     *Dehalococcoidales* ord. nov. and family *Dehalococcoidaceae* fam. nov., within the phylum

395     *Chloroflexi*. *Int. J. Syst. Evol. Microbiol.* **63**, 625-635 (2015).

396     (39)     Waller, A. S.; Krajmalnik-Brown, R.; Löffler, F. E.; Edwards, E. A. Multiple reductive-

397     dehalogenase-homologous genes are simultaneously transcribed during dechlorination by

398     *Dehalococcoides*-containing cultures. *Appl. Environ. Microbiol.* **71**, 8257-8264 (2005).

399     (40)     Puentes Jácome, L. A.; Edwards, E. A. A switch of chlorinated substrate causes

400     emergence of a previously undetected native *Dehalobacter* population in an established

401     *Dehalococcoides*-dominated chloroethene-dechlorinating enrichment culture. *FEMS Microbiol.*

402     *Ecol.* **93**, fix141 (2017).

403     (41)     Nelson, J. L.; Jiang, J.; Zinder, S. H. Dehalogenation of chlorobenzenes,

404     dichlorotoluenes, and tetrachloroethene by three *Dehalobacter* spp. *Environ. Sci. Technol.* **48**,

405     3776-3782 (2014).

(42)     Alfán-Guzmán, R.; Ertan, H.; Manefield, M.; Lee, M. Isolation and characterization of

*Dehalobacter* sp. strain TeCB1 including identification of TcbA: a novel tetra- and

trichlorobenzene reductive dehalogenase. *Front. Microbiol. 8*, 558 (2017).

(43)     Bao, Y. X.; Qu, Y. X.; Huang, J.; Cagnetta, G.; Yu, G.; Weber, R. First assessment on

degradability of sodium *p*-perfluorous nonenoxybenzene sulfonate (OBS), a high volume

alternative to perfluorooctane sulfonate in fire-fighting foams and oil production agents in China.

*RSC Adv. 7*, 46948-46957 (2017).

(44)     Washington, J. W.; Jenkins, T. M.; Weber, E. J. Identification of unsaturated and 2H

polyfluorocarboxylate homologous series and their detection in environmental samples and as

polymer degradation products. *Environ. Sci. Technol. 49*, 13256-13263 (2015).

(45)     Men, Y. J.; Feil, H.; VerBerkmoes, N. C.; Shah, M. B.; Johnson, D. R.; Lee, P. K. H.;

West, K. A.; Zinder, S. H.; Andersen, G. L.; Alvarez-Cohen, L. Sustainable syntrophic growth of

*Dehalococcoides ethenogenes* strain 195 with *Desulfovibrio vulgaris Hildenborough* and

*Methanobacterium congolense*: global transcriptomic and proteomic analyses. *ISME J. 6*, 410-

421 (2012).

(46)     He, J.; Holmes, V. F.; Lee, P. K.; Alvarez-Cohen, L. Influence of vitamin $B_{12}$ and

cocultures on the growth of *Dehalococcoides* isolates in defined medium. *Appl. Environ.

Microbiol. 73*, 2847-2853 (2007).

(47)     Yu, Y. C.; Han, P.; Zhou, L. J.; Li, Z.; Wagner, M.; Men, Y. J. Ammonia

monooxygenase-mediated cometabolic biotransformation and hydroxylamine-mediated abiotic

transformation of micropollutants in an AOB/NOB coculture. *Environ. Sci. Technol. 52*, 9196-

9205 (2018).

428    (48)    Zhou, L. J.; Han, P.; Yu, Y.; Wang, B.; Men, Y.; Wagner, M.; Wu, Q. L. Cometabolic

429    biotransformation and microbial-mediated abiotic transformation of sulfonamides by three

430    ammonia oxidizers. *Water Res.* **159**, 444-453 (2019).

431    (49)    Men, Y.; Han, P.; Helbling, D. E.; Jehmlich, N.; Herbold, C.; Gulde, R.; Onnis-Hayden,

432    A.; Gu, A. Z.; Johnson, D. R.; Wagner, M.; Fenner, K. Biotransformation of two

433    pharmaceuticals by the ammonia-oxidizing archaeon *Nitrososphaera gargensis*. *Environ. Sci.*

434    *Technol.* **50**, 4682-4692 (2016).

435    (50)    Becke, A. D. Density-functional thermochemistry. III. The role of exact exchange. *J.*

436    *Chem. Phys.* **98**, 5648-5652 (1993).

437    (51)    Lee, C.; Yang, W.; Parr, R. G. Development of the Colle-Salvetti correlation-energy

438    formula into a functional of the electron density. *Phys. Rev. B* **37**, 785-789 (1988).

439    (52)    Stephens, P.; Devlin, F.; Chabalowski, C.; Frisch, M. J. Ab initio calculation of

440    vibrational absorption and circular dichroism spectra using density functional force fields. *J.*

441    *Phys. Chem.* **98**, 11623-11627 (1994).

442    (53)    Vosko, S. H.; Wilk, L.; Nusair, M. Accurate spin-dependent electron liquid correlation

443    energies for local spin density calculations: a critical analysis. *Can. J. Phys.* **58**, 1200-1211

444    (1980).

445    (54)    Grimme, S.; Ehrlich, S.; Goerigk, L. Effect of the damping function in dispersion

446    corrected density functional theory. *J. Comput. Chem.* **32**, 1456-1465 (2011).

447    (55)    Marenich, A. V.; Cramer, C. J.; Truhlar, D. G. Universal solvation model based on solute

448    electron density and on a continuum model of the solvent defined by the bulk dielectric constant

449    and atomic surface tensions. *J. Phys. Chem. B* **113**, 6378-6396 (2009).

450  (56)    Livak, K. J.; Schmittgen, T. D. Analysis of relative gene expression data using real-time

451  quantitative PCR and the $2^{-\Delta\Delta CT}$ method. *Methods* **25**, 402-408 (2001).

452  (57)    Mei, R.; Narihiro, T.; Nobu, M. K.; Kuroda, K.; Liu, W. T. Evaluating digestion

453  efficiency in full-scale anaerobic digesters by identifying active microbial populations through

454  the lens of microbial activity. *Sci Rep.* **6**, 34090 (2016).

455  (58)    Sonthiphand, P.; Neufeld, J. D. Evaluating primers for profiling anaerobic ammonia

456  oxidizing bacteria within freshwater environments. *PLoS One* **8**, e57242 (2013).

457  (59)    Seshadri, R.; Adrian, L.; Fouts, D. E.; Eisen, J. A.; Phillippy, A. M.; Methe, B. A.; Ward,

458  N. L.; Nelson, W. C.; Deboy, R. T.; Khouri, H. M.; Kolonay, J. F.; Dodson, R. J.; Daugherty, S.

459  C.; Brinkac, L. M.; Sullivan, S. A.; Madupu, R.; Nelson, K. T.; Kang, K. H.; Impraim, M.; Tran,

460  K.; Robinson, J. M.; Forberger, H. A.; Fraser, C. M.; Zinder, S. H.; Heidelberg, J. F. Genome

461  sequence of the PCE-dechlorinating bacterium *Dehalococcoides ethenogenes*. *Science* **307**, 105-

462  108 (2005).

463  (60)    MaymoGatell, X.; Chien, Y. T.; Gossett, J. M.; Zinder, S. H. Isolation of a bacterium that

464  reductively dechlorinates tetrachloroethene to ethene. *Science* **276**, 1568-1571 (1997).

465  (61)    Holmes, V. F.; He, J. Z.; Lee, P. K. H.; Alvarez-Cohen, L. Discrimination of multiple

466  *Dehalococcoides* strains in a trichloroethene enrichment by quantification of their reductive

467  dehalogenase genes. *Appl. Environ. Microbiol.* **72**, 5877-5883 (2006).

468  (62)    Grostern, A.; Edwards, E. A. Characterization of a *Dehalobacter* coculture that

469  dechlorinates 1,2-dichloroethane to ethene and identification of the putative reductive

470  dehalogenase gene. *Appl. Environ. Microbiol.* **75**, 2684-2693 (2009).

471

472

**SUPPLEMENTARY MATERIALS:**

Materials and Methods

Tables S1−S3

Figs. S1−S27

References (*45-62*)

# Supplementary Materials for

## Microbial cleavage of C–F bonds in per- and polyfluoroalkyl substances via dehalorespiration

Yaochun Yu, Kunyang Zhang, Zhong Li, Changxu Ren, Jinyong Liu, Yujie Men[*]

[*]Correspondence to: ymen2@illinois.edu

**This PDF file includes:**

**Table of Content**

1    **Materials and Methods**

2    **Chemicals.** Standard compounds of perfluoro-n-octanoic acid (CAS number: 335-67-1, PFOA),

3    perfluoro-3,7-dimethyloctanoic acid (CAS number: 172155-07-6, PFdiMeOA), (E)-perfluoro(4-

4    methylpent-2-enoic acid) (CAS number: 103229-89-6, PFMeUPA), 4,5,5,5-tetrafluoro-4-

5    (trifluoromethyl)-2-pentenoic acid (CAS number: 243139-64-2, FTMeUPA), 4,5,5,5-tetrafluoro-

6    4-(trifluoromethyl) pentanoic acid (CAS number: 243139-62-0, FTMePA), and 3-

7    (trifluoromethyl)-3,4,4,4-tetrafluorobutene-1 (CAS number: 88562-41-8, polyfluorobutene) were

8    purchased form Synquest Laboratories and used without further purification. For PFOA,

9    PFdiMeOA, PFMeUPA, FTMeUPA, and FTMePA, 10 mM stock solutions of each standard were

10   prepared anaerobically in autoclaved Milli-Q water in 160 mL sealed serum bottles and stored at

11   room temperature until use. For the polyfluorobutene, methanol was used to dissolve the

12   compound for $MS^2$ analysis.

13   **Cultures and growth conditions.** The *Dehalococcoides*-containing TCE-dechlorinating

14   enrichment (KB1) was generously provided by SiREM Lab (https://www.siremlab.com/). Pure

15   *Dehalococcoides mccartyi* BAV1 (ATCC BAA-2100) and FL2 (ATCC BAA-2098) were

16   purchased from American Type Culture Collection (ATCC). Pure *Dehalobacter restrictus* was

17   purchased from DSMZ (DSM-9455). All cultures were maintained in 160 mL sealed serum

18   bottles containing 100 mL sterile anaerobic basal medium with 100 μg/L vitamin $B_{12}$ as

19   previously described *(45, 46)* and 60 mL Ar/$CO_2$ headspace. For the maintenance of KB1

20   culture, 5 mM lactate and 2 μL neat TCE (ca. 220 μM) were added as electron donor and

21 electron acceptor, respectively, and were re-added periodically. For *Dehalococcoides mccartyi*

22 BAV1, 5 mM acetate, 2 μL neat *cis*-DCE were supplied upon depletion. For *Dehalococcoides*

23 *mccartyi* FL2 and *Dehalobacter restrictus*, 5 mM acetate, 2 μL neat TCE were supplied upon

24 depletion. $H_2/Ar/CO_2$ headspace was used for the three dechlorinating pure cultures. All cultures

25 were incubated at 34 °C in a dark incubator without shaking.

26 **Biodefluorination experiments.** Ten mL of the dechlorinating enrichment or pure culture was

27 inoculated into 90 mL sterile fresh medium as described above. The electron acceptor was added

28 in three scenarios: (1) 75 μM individual PFAS species as the sole electron acceptor; (2) 75 μM

29 PFAS with 220 μM TCE (or *cis*-DCE for BAV1) as the co-substrate, and TCE/*cis*-DCE was re-

30 added upon depletion; (3) 220 μM TCE/*cis*-DCE as the sole electron acceptor with reamendment

31 upon depletion as culture activity control. Headspace and aqueous samples were taken

32 subsequently during the incubation period for the measurement of chloroethenes, PFASs and $F^-$.

33 Briefly, four mL culture suspension was centrifuged at 16,000 $\times$ $g$ (4 °C for 30 min). Two mL

34 supernatant was used for $F^-$ measurement. The rest 2 mL was collected for LC-HRMS/MS

35 measurement. Cell pellets were stored properly for DNA ($-$ 20 °C) and RNA ($-$ 80 °C)

36 extraction, respectively. Heat-inactivated biomass (two cycles of autoclavation at 121 °C for 20

37 min) control and biomass-free sterile fresh medium control were set up in the same way as

38 described above, both controls were amended with the same nutrients. All experimental groups

39 and controls were set up in triplicates.

40 **Fluoride ion measurement.** The concentration of fluoride ion ($F^-$) in culture supernatant was

41  determined by an ion selective electrode (ISE, HACH, Loveland, CO) connected with a HQ30D

42  Portable Multi Meter (HACH). A 100 μg fluoride ionic strength adjustment powder (HACH) was

43  added into 2 mL culture supernatant, and the F⁻ concentration was then measured with the ISE-

44  Multi Meter system. The ISE was calibrated each time before sample measurement according to

45  manufacturer's instructions. In addition, ion chromatography (IC) was used to validate the

46  fluoride measurement by ISE. The two methods exhibited consistent fluoride concentrations in

47  the tested samples.

48  **Gas chromatography coupled to mass selective detector (GC-MSD) analysis.** Chlorinated

49  ethenes and ethene in all experimental samples fed with TCE/*cis*-DCE were regularly measured

50  by injecting 500 μL headspace sample into a GC-MSD (6850 Network GC system, 5975C VL

51  MSD, Agilent, Santa Clara, CA) equipped with a Rtx-200 capillary column (30 m × 250 μm ×

52  1 μm; Shimadzu, Columbia, MD). The oven temperature was programmed to hold at 45 °C for 1

53  minute, increased to 200 °C in 3.44 minutes, and hold at 200 °C for 1 minute. The temperatures

54  of injector and detector were maintained at 220 °C and 250 °C, respectively.

55  **High-performance liquid chromatography coupled to high-resolution tandem mass**

56  **spectrometry (HPLC-HRMS/MS) analysis.** Concentrations of parent compound and

57  transformation products were analyzed by high performance liquid chromatography coupled to a

58  high-resolution quadrupole orbitrap mass spectrometer (HPLC-HRMS/MS, Q Exactive, Thermo

59  Fisher Scientific, Waltham, MA) in the Metabolomics Lab of Roy J. Carver Biotechnology

60  Center at University of Illinois at Urbana-Champaign. For HPLC analysis, a 50 μL sample were

61    loaded onto a Zorbax SB-Aq column (particle size 5μm, 4.6×50 mm, Agilent), and eluted with

62    10 mM ammonia formate (A) and methanol (B) at a flow rate of 350 μL/min. The linear gradient

63    for LC separation was set as: 100% A for 0 − 1 min, 100% − 2% A for 2 − 15 min, 2% − 100 %

64    A in 1 min, and 100% A for 16 − 21 min. For HRMS, mass spectra were acquired in full scan

65    mode at a resolution of 70,000 at m/z 200 and a scan range of m/z 50 − 750 under

66    negative/positive switch ionization (ESI) mode. The Xcalibur 4.0 and TraceFinder 4.1 EFS

67    (Thermo Fisher Scientific) were used for data acquisition and analysis. The limit of

68    quantification (LOQ) for each investigated compound is determined as the lowest concentration

69    of calibration standards with a detection variation < 20%, which was listed in Table S1.

70    **Transformation product (TP) identification.** Both suspect screening and nontarget screening

71    were conducted to identify transformation products as previously described *(47, 48)*. Suspect

72    screening was done by TraceFinder 4.1 EFS and Xcalibur 4.0 software (Thermo Fisher

73    Scientific). TP suspect lists were generated by an automated metabolites mass prediction script

74    *(49)*, which was modified to specifically predict the defluorination products via different

75    biological reaction pathways including a number of known reduction reactions, hydrolysis

76    reactions, and conjugation reactions at both primary and secondary levels. Plausible

77    transformation products were selected based on the following criteria: (i) mass accuracy

78    tolerance < 5 ppm; (ii) isotopic pattern score > 90%; (iii) peak area > $10^8$; (iv) increasing trend

79    along time or first increase then decrease; (v) no formation in heat-inactivated controls and

80    absent in biological samples without any PFAS addition. For non-target screening, software

7

81   Sieve 2.2 (Thermo Fisher Scientific) was used for data analysis. The potential TPs were selected

82   based on the same criteria as suspect screening. For TPs with authentic standards, MS$^2$ fragment

83   profiles of both standard compounds and TP candidates were acquired using data-dependent MS$^2$

84   scan based on the exact mass of the precursor ion to elucidate the structures of TPs. MS$^2$

85   fragment profiles of TPs without available authentic standards were compared with the predicted

86   fragments by Competitive Fragmentation Modeling for Metabolite Identification (CFM-ID,

87   http://cfmid.wishartlab.com/).

88   **Bond dissociation energy (BDE) calculation.** GAUSSIAN 09 quantum chemistry package was

89   used to obtain the C−F BDEs for the parent and daughter PFASs examined in Fig. 3 and 4. All

90   molecular structures were optimized at the B3LYP/6-311+G(2d,2p) level of theory *(50-53)*.

91   Grimme's empirical dispersion correction with Becke-Johnson damping (GD3-BJ) was

92   employed to approximate the dispersion interaction between molecules *(54)*. The SMD

93   continuum solvation model was selected to simulate the solvent effect implicitly *(55)*. Frequency

94   examinations of all optimized geometries were done to confirm that the local minima were

95   reached instead of obtaining the first-order saddle point. The BDE for each C−F bond was

96   calculated through a previously reported formula:

97   $$BDE = \left(H^*_{radical[PFASminusF]} + H^*_{radicalF}\right) - H^*_{parentPFAS}$$

98   where $H^*$ represents the enthalpy of formation *(10)*.

99   **DNA extraction and quantitative polymerase chain reaction (qPCR).** Biomass from 0.5 mL

100   culture were sampled from each biological replicate. Microbial genomic DNA was extracted by

101     DNeasy PowerSoil Kit (QIAGEN, Germantown, MD) according to manufacturer's instructions.

102     Cell growth was measured by qPCR using primers targeting universal bacterial 16S rRNA genes,

103     and 16S rRNA genes of *Dehalococcoides* spp., *Dehalobacter* spp., and *Geobacter* spp. (Table

104     S3). Genomic DNA of *Dehalococcoides mccartyi* FL2 and *Dehalobacter restrictus* were

105     quantified by NanoDrop One (Thermo Fisher Scientific) and served as qPCR standards. The

106     relative abundance of reductive dehalogenase (RDH) genes was determined by qPCR using the

107     primers listed in Table S3. PowerUp SYBR Green reagents (Thermo Fisher Scientific) were used

108     for qPCR according to the manufacturer's instructions. Briefly, every 20-µL reaction mixture

109     contained 2.5 µL of gDNA sample or serially diluted standard, 10 µL of 2 × PowerUp SYBR

110     Green master mix solution, and 1.25 µL 10µM of forward and reverse primers. The PCR

111     procedure included an initial deactivation at 95 °C for 2 min, followed by 40 thermal cycles at

112     95 °C for 1 s, then at 60 °C for 30 s.

113     **Reverse-transcription qPCR (RT-qPCR).** RNA was extracted using acid-phenol: chloroform:

114     isoamyl alcohol (25: 24: 1), and precipitated in ethanol at – 20 °C as described previously *(49)*.

115     RNA was cleaned up using the RNeasy PowerClean Pro CleanUp Kit (QIAGEN) according to

116     the manufacturer's instructions. Contaminating DNA in the RNA samples was removed by Turbo

117     DNase Kit (Thermo Fisher Scientific) following the manufacturer's instructions. qPCR was

118     carried out to verify the removal of genomic DNA contamination from the purified RNA. The

119     quality of RNA was examined by agarose gel electrophoresis.

120     SuperScript III First-Strand Synthesis System (Thermo Fisher Scientific) was applied for

121    cDNA synthesis according to the manufacturer's instructions. In general, the 10 μL cDNA

122    synthesis mix containing 8 μL of RNA sample, 1 μL of primer and 1 μL of 10 mM dNTP mix

123    was incubated at 65 °C for 5 min, then placed on iced for 1 min. The cDNA synthesis mix was

124    added to each RNA/primer mixture and incubated at 25 °C for 10 min then 50 °C for 50 min.

125    The reaction was terminated at 85 °C for 5 min, then the entire tube was chilled on ice. At last, 1

126    μL of RNase H was added to each tube and incubated at 37 °C for 20 min. The cDNA synthesis

127    products were stored at – 20 °C for qPCR measurement using primers listed in Table S3.

128        Double delta Ct method (calculated by Equation 1) was used to determine the relative gene

129    expression of RDH genes with *Dehalococcoides* 16S rRNA gene as the reference gene *(56)*.

130    Equation: Fold Change of Transcript Abundance $= 2^{-\Delta\Delta Ct}$, where

131    $\Delta\Delta Ct = \Delta Ct_{PAFS-added\ sample} - \Delta Ct_{TCE-only\ control}$, $\Delta Ct = Ct_{RDH\ gene} - Ct_{16S\ rRNA\ gene}$

132

**Table S1.** Standards and TPs information
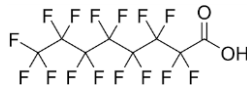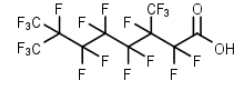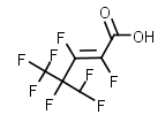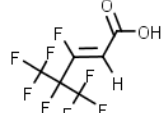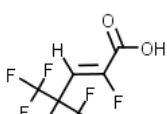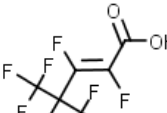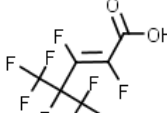
| Compound ID | Formula | [M−H]⁻ | Observed Fragments | Predicted Fragments | Structure | LOQ (μM) |
|---|---|---|---|---|---|---|
| PFOA | $C_8HF_{15}O_2$ | 412.9664 | **368.9765**; 218.9858; 168.9883; 118.9914 | **368.9766**; 268.9830 |  | 0.01 |
| PFdiMeOA | $C_{10}HF_{19}O_2$ | 512.9600 | **468.9706**; **318.9804**; 268.9833; 218.9854; 168.9883; 118.9912 | **468.9702**; **318.9798**; 68.9958 |  | 0.01 |
| PFMeUPA | $C_6HF_9O_2$ | 274.9760 | **230.9859**; 180.9892; 68.9942 | **230.9862**; 168.9894 |  | 0.01 |
| **TP256** | $C_6H_2F_8O_2$ | 256.9854 | **212.9952**; **192.9887**; **168.9884** | **212.9956**; **192.9894**; **168.9894** |  | |
| | | | | 236.9792; **212.9956**; **192.9894**; 186.9824; **168.9894**; 142.9926 |  | n.a. |
| | | | | 236.9792; **212.9956**; **192.9894**; 150.9988 |  | |
| | | | | 236.9792; **212.9956**; **192.9894**; 150.9988; 106.9950 |  | n.a. |

11

**Table S1.** Standards and TPs information (continue)
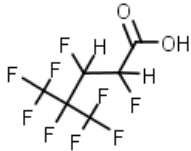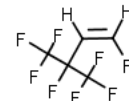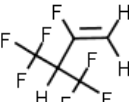
| Compound ID | Formula | [M−H]⁻ | Observed | Predicted | Structure | LOQ (µM) |
|---|---|---|---|---|---|---|
| **TP276** | C₆H₃F₉O₂ | 276.9917 | **212.9949**; 192.9886 | 258.9811; 256.9854; 233.0018; 230.9862; **212.9956**; 206.9886; 168.9894; 162.9988 |  | n.a. |
| **TP212** | C₅H₂F₈ | 212.9952 | **192.9887; 168.9884** | **192.9894; 168.9894** |  | n.a. |
| | | | | **192.9894; 168.9894;** 142.9926 |  | |
| 3-(Trifluoromethyl)-3,4,4,4-tetrafluorobutene-1 | C₅H₃F₇ | 195.0043 | n.d. | 174.9988; 168.9894; 154.9926; 125.0020; 104.9958 |  | n.a. |
| **TP195** | C₅H₃F₇ | 195.0043 | **174.9980; 154.9915** | **174.9988; 154.9926;** 150.9987; 130.9926 |  | n.a. |
| | | | | **174.9988; 154.9926;** 150.9988; 130.9926; 125.0020; 104.9957 |  | |

**Table S1.** Standards and TPs information (continue)
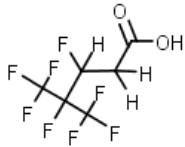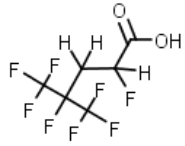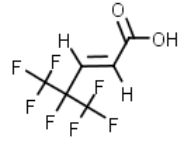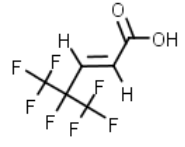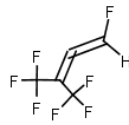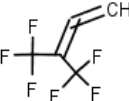
| Compound ID | Formula | [M−H]⁻ | Observed | Predicted | Structure | LOQ (µM) |
|---|---|---|---|---|---|---|
| **TP259** | $C_6H_4F_8O_2$ | 259.0011 | **238.9951**; **195.0043**; 174.9960; **168.9985**; 154.9915 | 240.9905; **238.9949**; 215.0112; 212.9956; **195.0050**; 188.9980; 170.9875; **168.9918**; 145.0082 <br><br> 240.9905; **238.9949**; 215.0112; 212.9956; **195.0050**; 188.9980; 170.9875; **168.9918**; 145.0082 |  | n.a. |
| **TP238** (FTMeUPA) | $C_6H_3F_7O_2$ | 238.9949 | **218.9879**; **198.9815**; **174.9977**; **168.9883**; 154.9913; 132.9895 | 220.9843; **218.9886**; **198.9824**; 195.0050; 192.9894; **174.9988**; **168.9894**; 148.9856; 125.0020 |  | 0.01 |
| TP192 | $C_5HF_7$ | 192.9881 | no fragment | no fragment |  | n.a. |
| TP174 | $C_5H_2F_6$ | 174.9974 | **154.9915** | **154.9926** |  | n.a. |

| Compound ID | Formula | [M−H]⁻ | Observed | Predicted | Structure | LOQ (µM) |
|---|---|---|---|---|---|---|
| TP154 | $C_5HF_5$ | 154.9915 | no fragment | no fragment |  | n.a. |
| **TP241**(FTMePA) | $C_6H_5F_7O_2$ | 241.0105 | **221.0059;** **200.9978;** 180.9911; **177.0137** | 222.9999; **221.0043;** 202.9934; **200.9980;** 197.0203; **177.0144** |  | 0.01 |
| **TP221** | $C_6H_4F_6O_2$ | 221.0043 | **200.9974;** **180.9910;** 152.9958; **132.9895;** **130.9917;** 108.9893; **104.9943** | 202.9937; **200.9980;** 182.9875; **180.9918;** 177.0144; 174.9988; 168.9918; 157.0082; 154.9926; 151.0012; **132.9907;** **130.9926;** 125.0020; 107.0114; **104.9958** |  | n.a. |
| | | | **200.9974;** **180.9910;** 152.9958; 132.9895; **130.9917;** 108.9893; 104.9943 | 202.9937; **200.9980;** 182.9875; **180.9918;** 177.0144; 174.9988; 157.0082; 154.9926; 151.0012; **130.9926;** 107.0114 |  | n.a. |
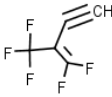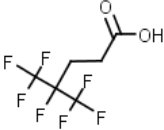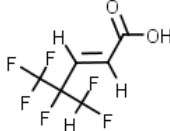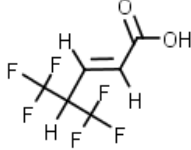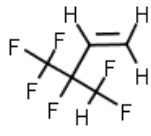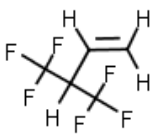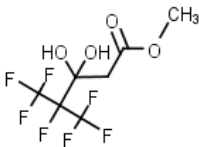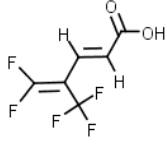
**Table S1.** Standards and TPs information (continue)

| Compound ID | Formula | [M−H]⁻ | Observed | Predicted | Structure | LOQ (μM) |
|---|---|---|---|---|---|---|
| **TP177** | $C_5H_4F_6$ | 177.0133 | **137.0008**; 116.9944 | 157.0082; 150.9988; **137.0020**; 130.9926; 125.0020; 107.0114; 104.9958 |  | n.a. |
| | | | | 157.0082; 150.9988; **137.0020**; 130.9926; 107.0114 |  | |
| TP287 | $C_7H_7F_7O_4$ | 287.0163 | **241.0106**; 206.3808; 200.9973; 180.9911; 177.0137 | 269.0054; 254.9898; **241.0105**; 229.0105; 210.9999; 196.9843; 168.9894; |  | n.a. |
| TP200 | $C_6H_3F_5O_2$ | 200.9978 | **180.9912**, 160.9850, 152.9960, 132.9896, 108.9894, | 182.9874, **180.9918**, 157.0082, 154.9926, 137.0019, 130.9950, 130.9926, 110.9887 |  | n.a. |

n.a.: not available; n.d.: not detected; TP names in **bold** are those with confirmed (confidence level 1) or highly plausible (confidence level 2b) structures.

**Table S2.** Comparison of selected PFASs ionization efficiency.

| Compound | Ionization efficiency ratio |
| --- | --- |
| FTMeUPA: PFMeUPA | 5.69 |
| FTMePA: PFMeUPA | 0.57 |
| FTMeUPA: FTMePA | 9.93 |

**Table S3.** Primer sets information.

| Gene target | Primer name | Sequence (5′-3′) | References |
|---|---|---|---|
| Universal bacteria 16S rRNA gene | Unibac_341f | CCTACGGGAGGCAGCAG | (57, 58) |
| | Unibac_518r | ATTACCGCGGCTGCTGG | |
| *Dehalococcoides* 16S rRNA gene | Dhc_f | GGTAATACGTAGGGAAGCAAGCG | (59-61) |
| | Dhc_r | CCGGTTAAGCCGGGAAATT | |
| *Dehalobacter* 16S rRNA gene | Dhb_447f | GATTGACGGTACCTAACGAGG | (62) |
| | Dhb_647r | TACAGTTTCCAATGCTTTACGG | |
| *Geobacter*_1 16S rRNA gene | Geo_f | CTTGCTCTTTCATTTAGTGG | (37) |
| | Geo_r | AAGAAAACCGGGTATTAACC | |
| rdhA1 | rdhA1_246f | ATCGGAGCTGCACAAGTAGG | (39) |
| | rdhA1_336r | TCTTGTGAGCGGTGTCTTTG | |
| rdhA2 | rdhA2_720f | CAAAGGAGATGTTCCGGTGT | (39) |
| | rdhA2_985r | CAGGTGGAAAAGACCGGTTA | |
| rdhA3 | rdhA3_1149f | CATTCTCCGGGAAGAAAACA | (39) |
| | rdhA3_1379r | CCAGGCTTCCTTGTCTTCAG | |
| rdhA4 | rdhA4_754f | TTGTTATGCCGCCAATATGA | (39) |
| | rdhA4_925r | TCTATCCATTTCGCCCAGAC | |
| rdhA5 | rdhA5_1017f | GATGCAGGCATTTACCGTTT | (39) |
| | rdhA5_1137r | GTCTCTTTGCCTTCGGTCAG | |
| rdhA6 | rdhA6_318f | ATTTAGCGTGGGCAAAACAG | (39) |
| | rdhA6_555r | CCTTCCCACCTTGGGTATTT | |
| rdhA7 | rdhA7_1391f | GCTAAAGAGCCGTCATCCTG | (39) |
| | rdhA7_1539r | GCAGTAACAACAGCCCCAAT | |
| rdhA8 | rdhA8_845f | CCCAAGGTAGGTGTGCAGAT | (39) |
| | rdhA8_1016r | CCCGGTTAGTTACCCCGTAT | |
| rdhA9 | rdhA9_251f | CTGACCTTGAAACCCCTGAA | (39) |
| | rdhA9_425r | TTGCCACCCATTTCCATATT | |
| rdhA10 | rdhA10_710f | GCTGAAACACCCACCAAACT | (39) |
| | rdhA10_860r | CGACAAAGGGGAATCTTTGA | |
| rdhA11 | rdhA11_429f | TAATGGCAACCGGAGGTAAG | (39) |
| | rdhA11_609r | TCTACCGGTATGGCCTGAAC | |
| rdhA12 | rdhA12_864f | AGGAGTTCCTGTGGGGACTT | (39) |
| | rdhA12_994r | TTTGGGGGTCATAACTGCTC | |
| rdhA13 | rdhA13_1356f | CAGGGTACCTGTCCCTTCAA | (39) |
| | rdhA13_1493r | AGGGTTCTTCCGTCCGTACT | |
| rdhA14 | rdhA14_642f | GAAAGCTCAGCCGATGACTC | (39) |
| | rdhA14_846r | TGGTTGAGGTAGGGTGAAGG | |

**Supplementary Figures.**
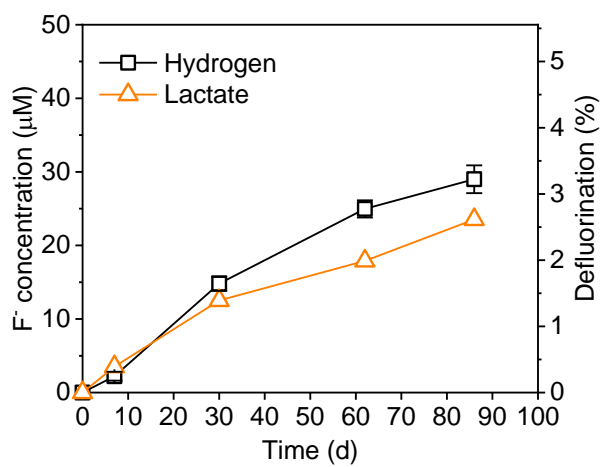


**Fig. S1.** Fluoride ion release from PFMeUPA (100 μM) with hydrogen/lactate as the primary

electron donor.
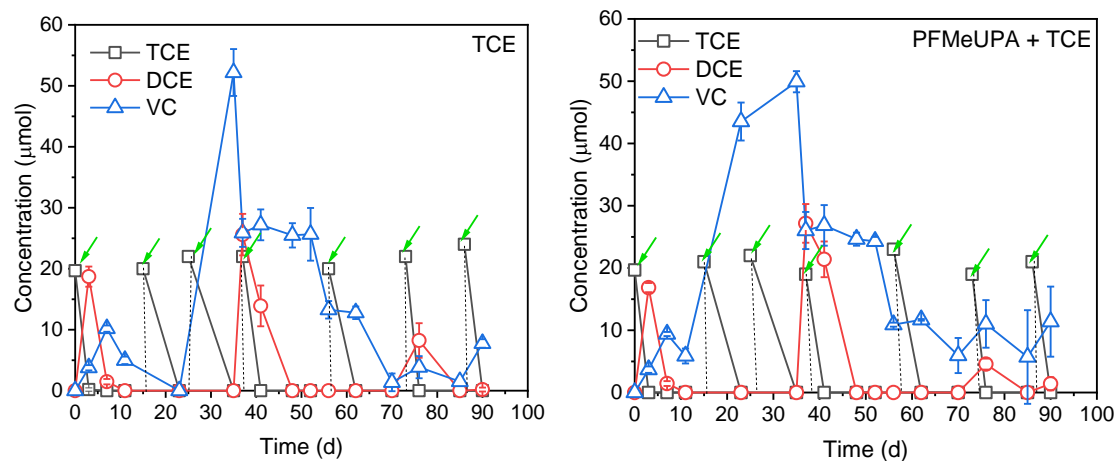
**Fig. S2**. TCE, *cis*-DCE, and VC in the culture with only TCE added (A) and the culture with both TCE and PFMeUPA added (B) (green arrows indicate the times when TCE was re-added).
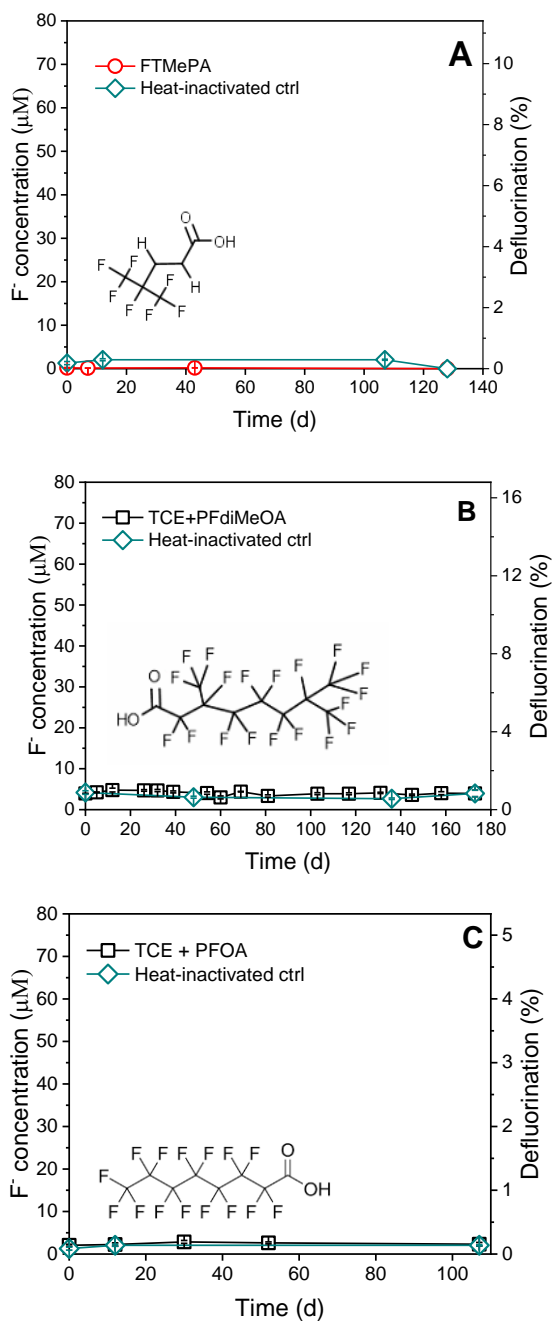
**Fig. S3**. Fluoride ion release from 100 μM of FTMePA (A), PFdiMeOA (B), and PFOA (C) in
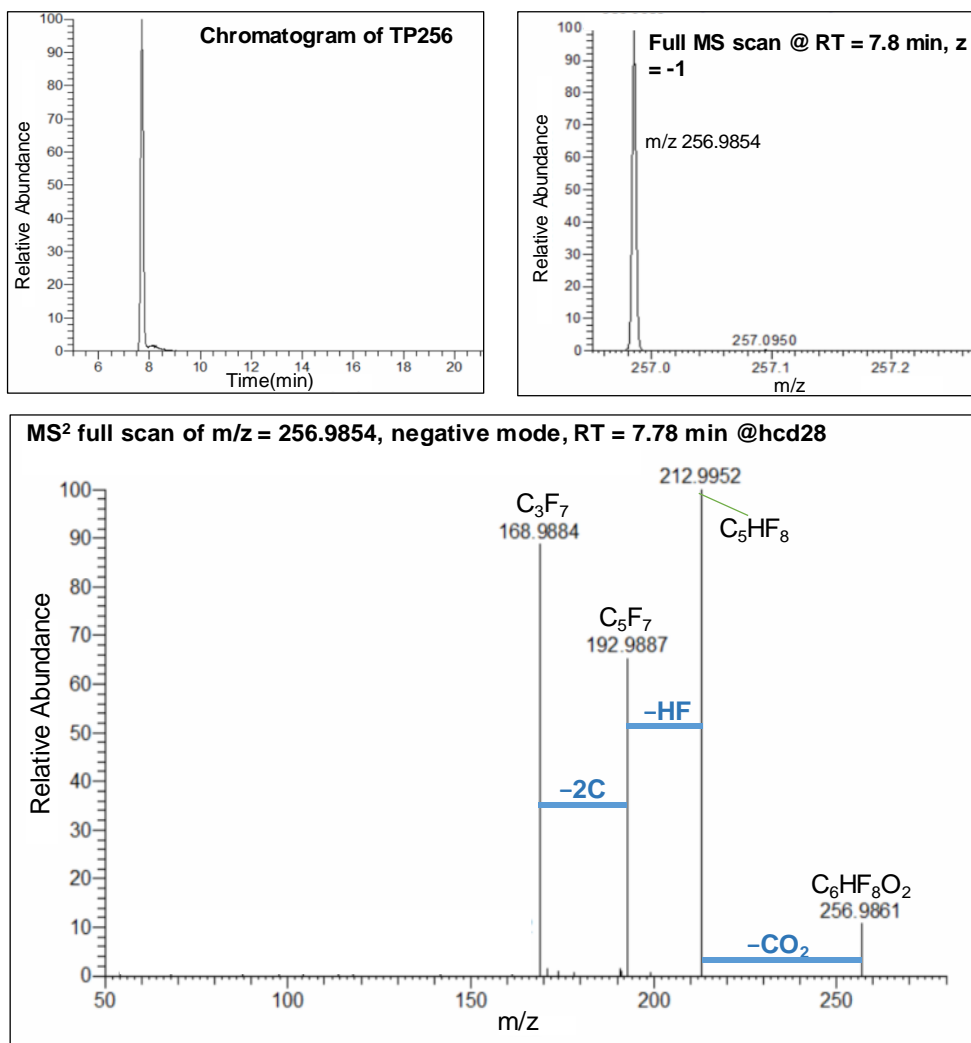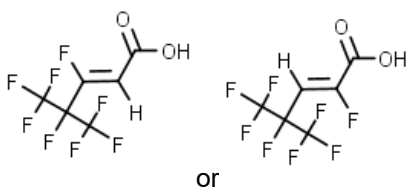
the dechlorinating microbial community.
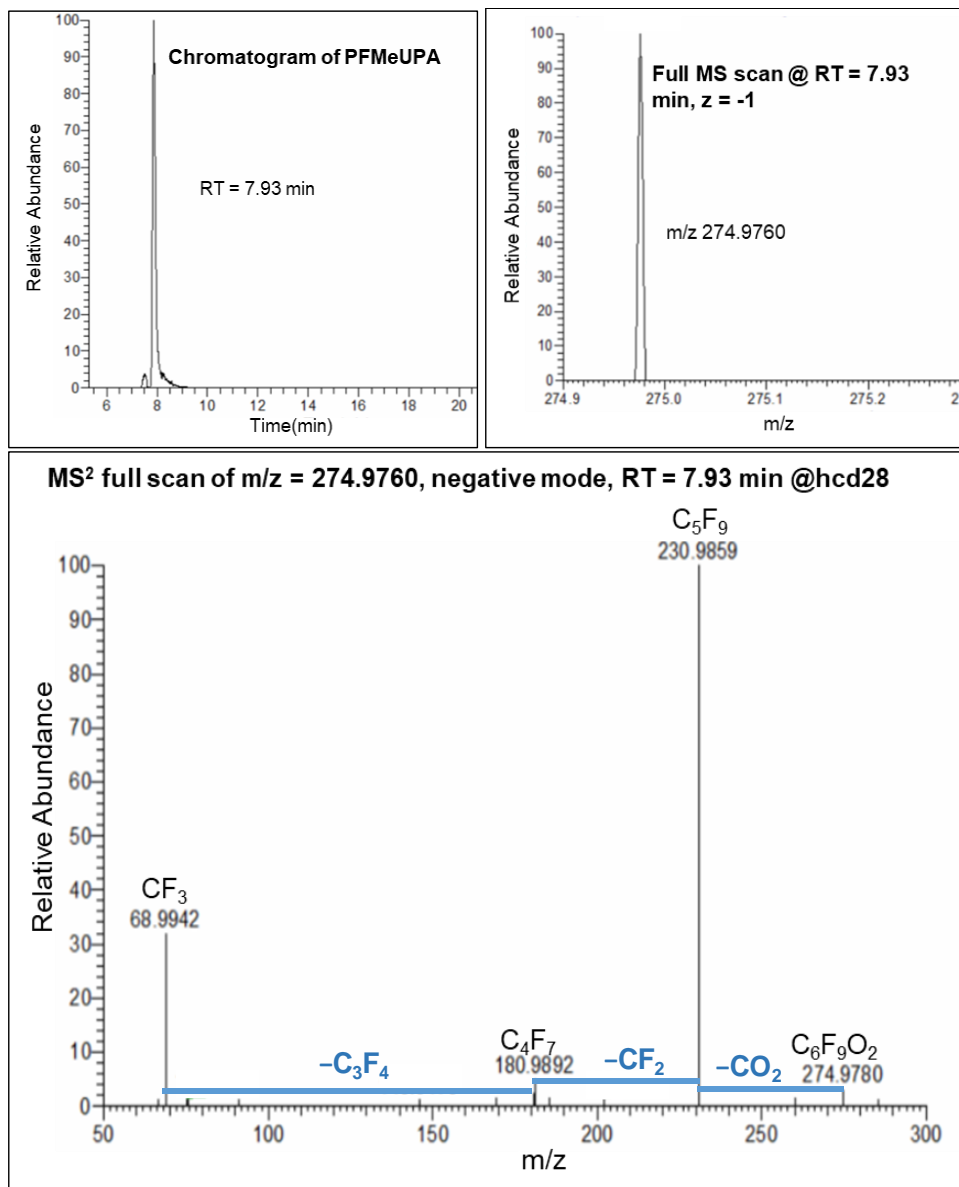
**Formula:** $C_6HF_9O_2$

**Structure:**
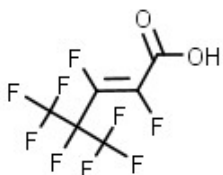


**Fig. S4.** $MS^2$ fragments of PFMeUPA

**Formula:** $C_6H_2F_8O_2$

**Atomic Modification:** −F +H of PFMeUPA

**Hypothetical Structure:**



or

**Confidence level:** 2b

**Fig. S5.** TP256 structure elucidation
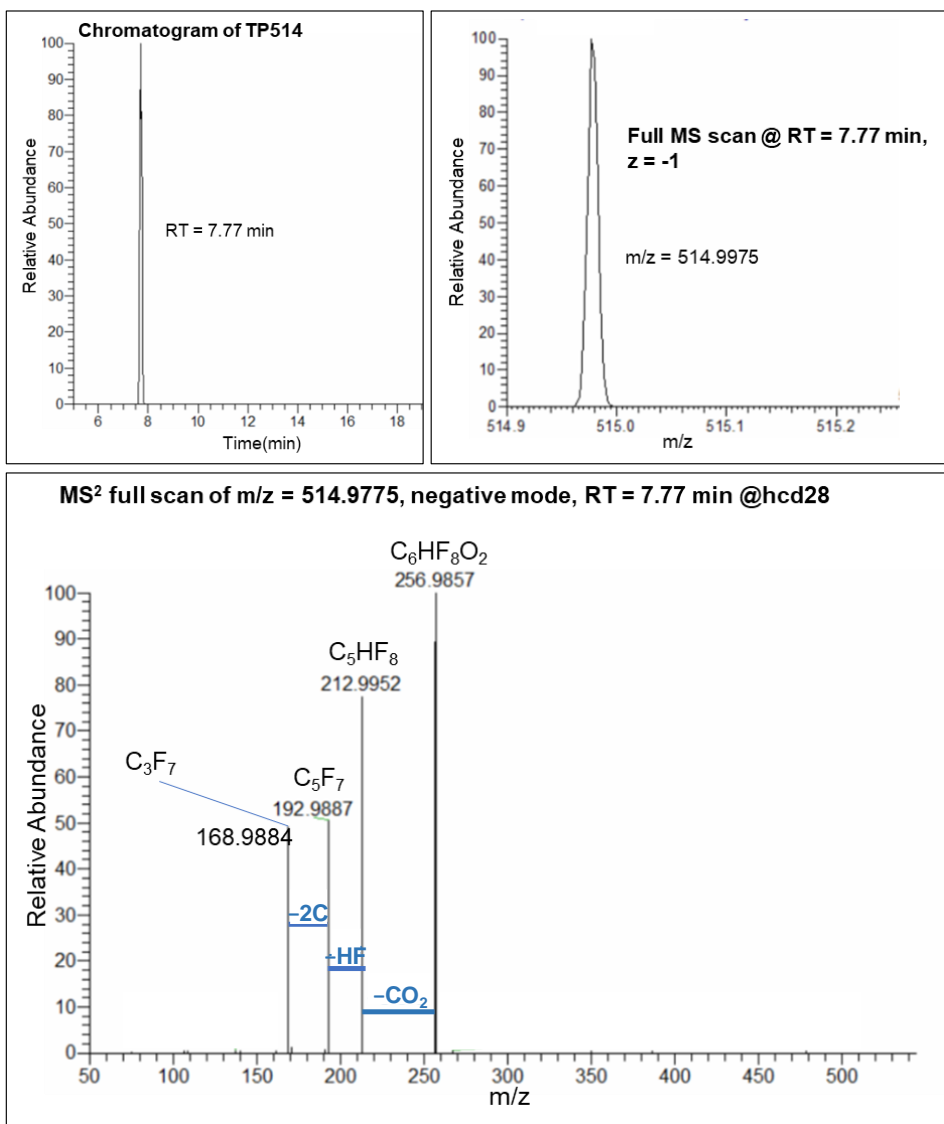
**Formula:** $C_{12}H_4F_8O_4$

**Atomic Modification:** Conjugate of two molecules of TP256

**Confidence level:** 2b

**Fig. S6**. TP514 structure elucidation
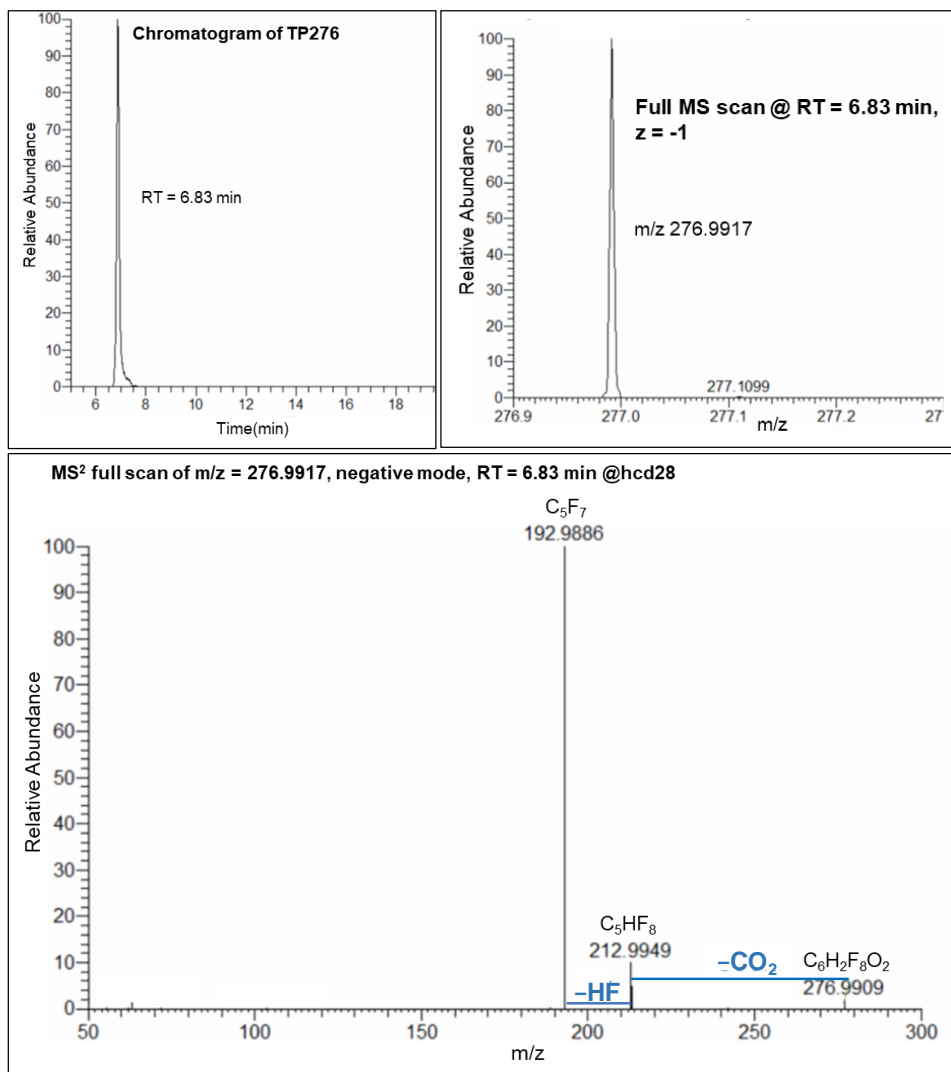
**Formula:** $C_6H_3F_8O_2$

**Atomic Modification:** +2H of PFMeUPA
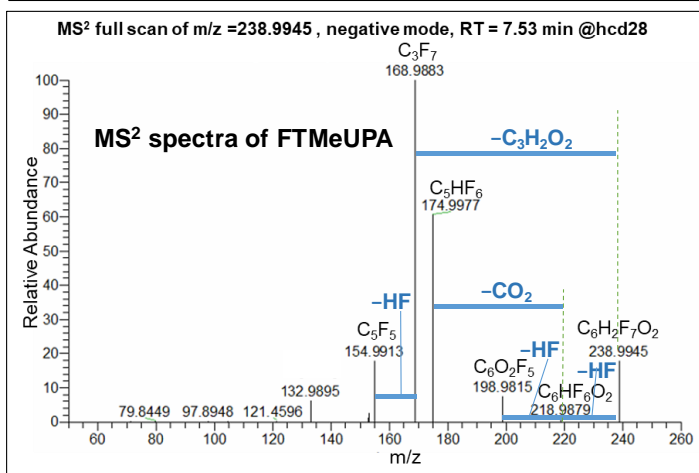
**Confidence level:** 2b

**Hypothetical Structure:**
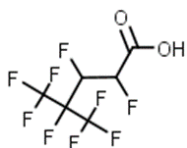


**Fig. S7**. TP276 structure elucidation
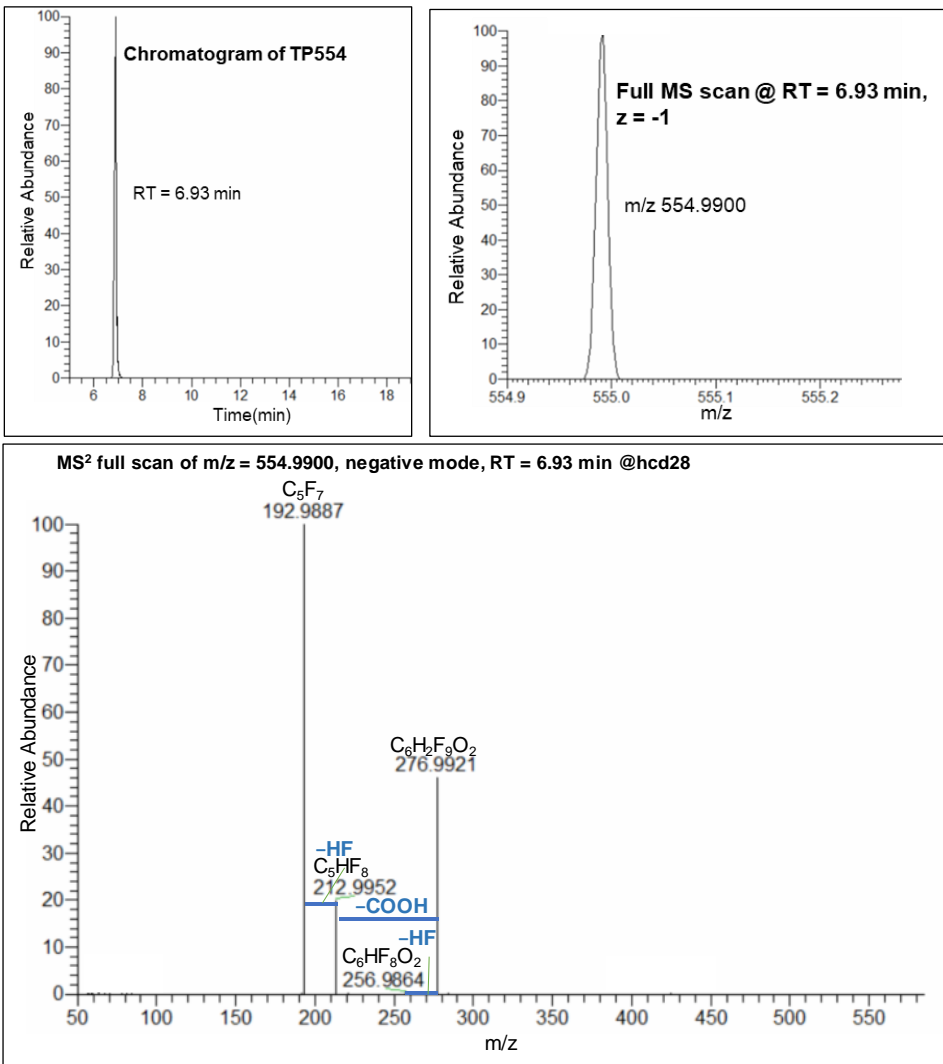
**Formula:** $C_{12}H_6F_{18}O_4$

**Atomic Modification:** Conjugate of two molecules of TP276

**Confidence level:** 2b

**Fig. S8**. TP554 structure elucidation

Fig. S9. TP259 structure elucidation

**Formula:** $C_6H_4F_8O_2$

**Atomic Modification:** −F +3H of PFMeUPA

**Confidence level:** 2b

**Hypothetical Structure:**
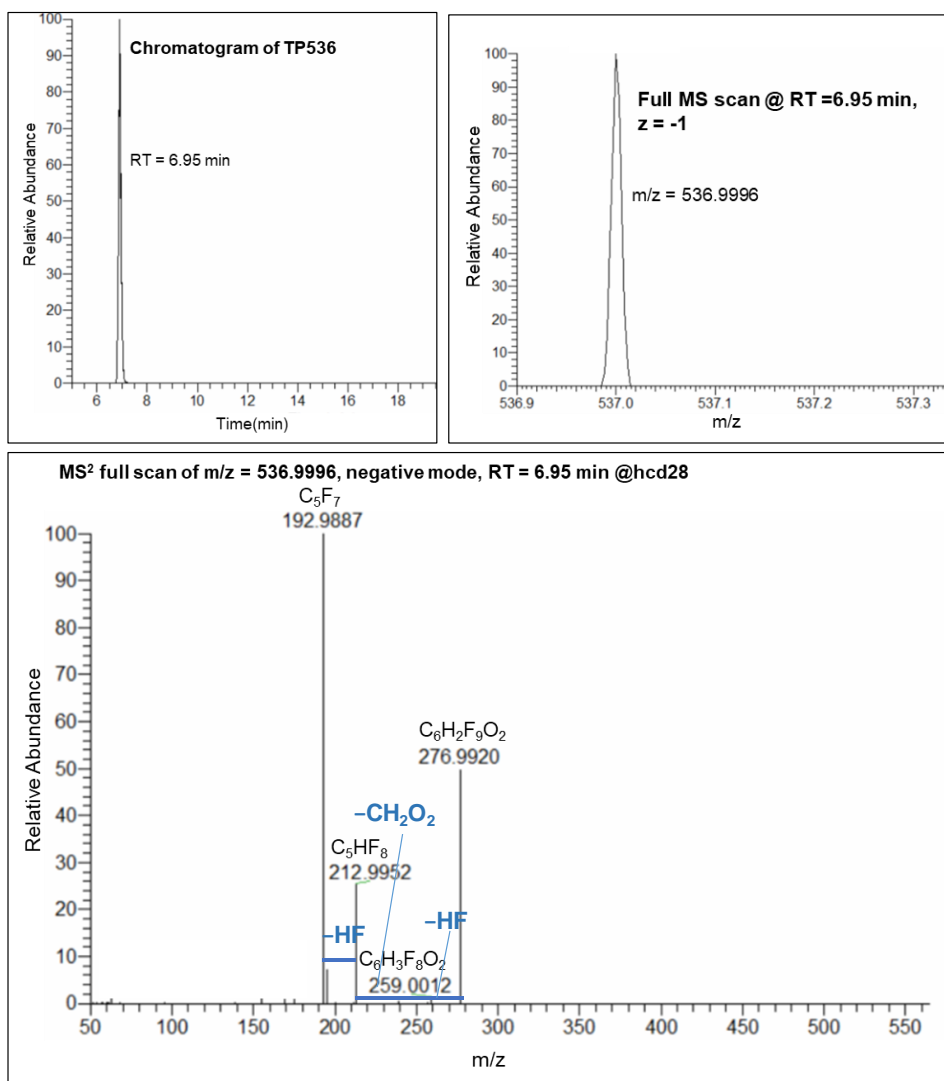
**Formula:** $C_{12}H_7F_{17}O_4$

**Atomic Modification:** Conjugate of TP259 and TP276

**Confidence level:** 2b

**Fig. S10.** TP536 structure elucidation
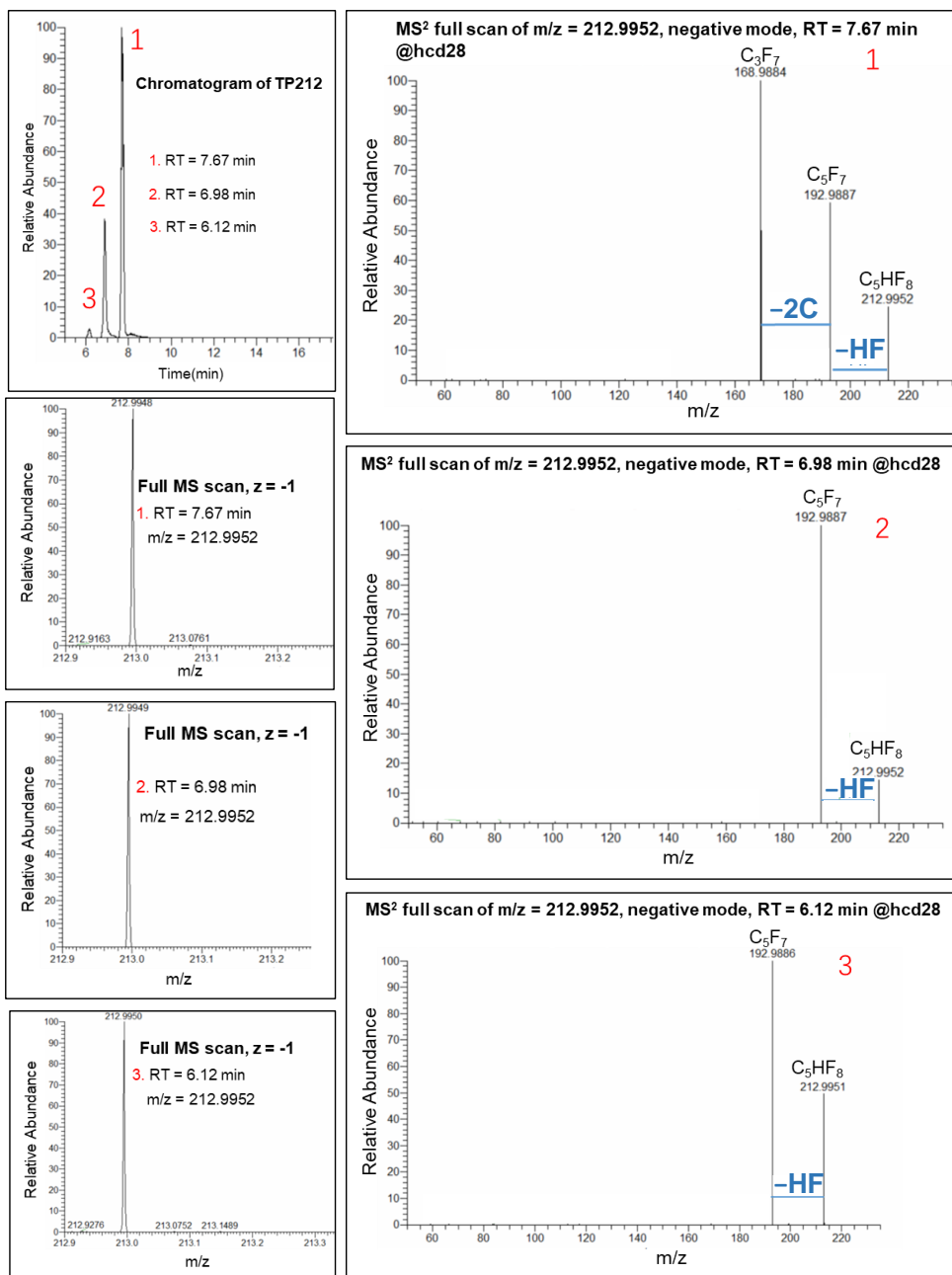
**Formula:** $C_5H_2F_8$

**Atomic Modification:** −F +H −$CO_2$ of PFMeUPA

**Confidence level:** 2b

**Hypothetical Structure:**
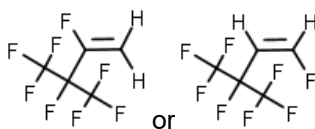


**Fig. S11.** TP212 structure elucidation
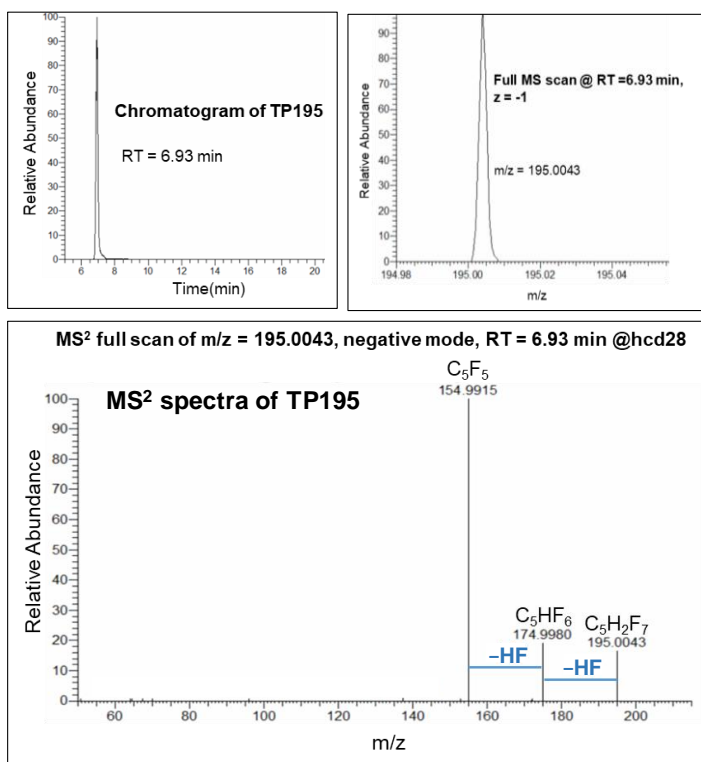
**Formula:** $C_5H_3F_7$

**Atomic Modification:** $-2F +2H -CO_2$ of PFMeUPA

**Hypothetical Structure:**



or
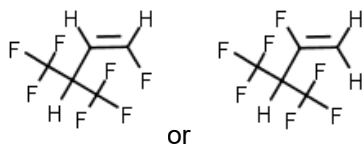
**Confidence level:** 2b

**Fig. S12.** TP195 structure elucidation
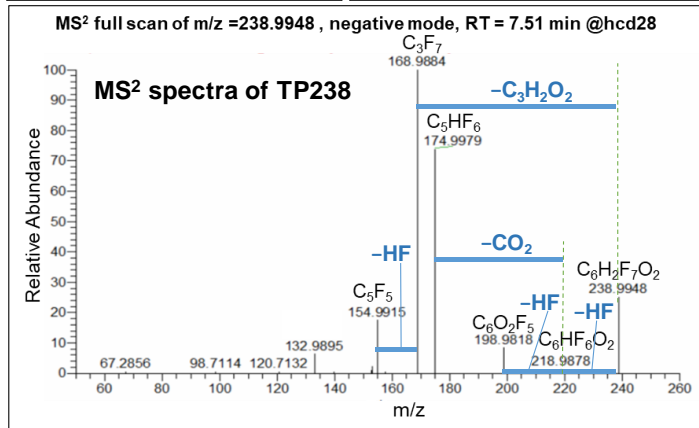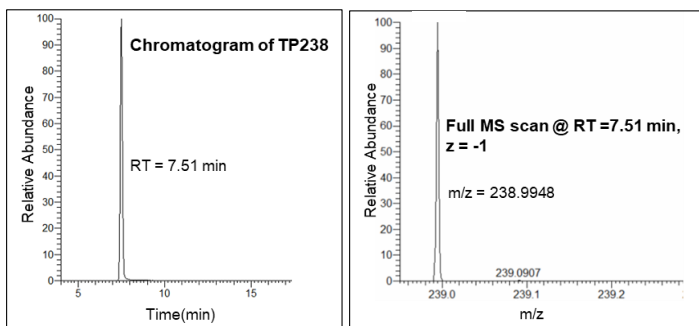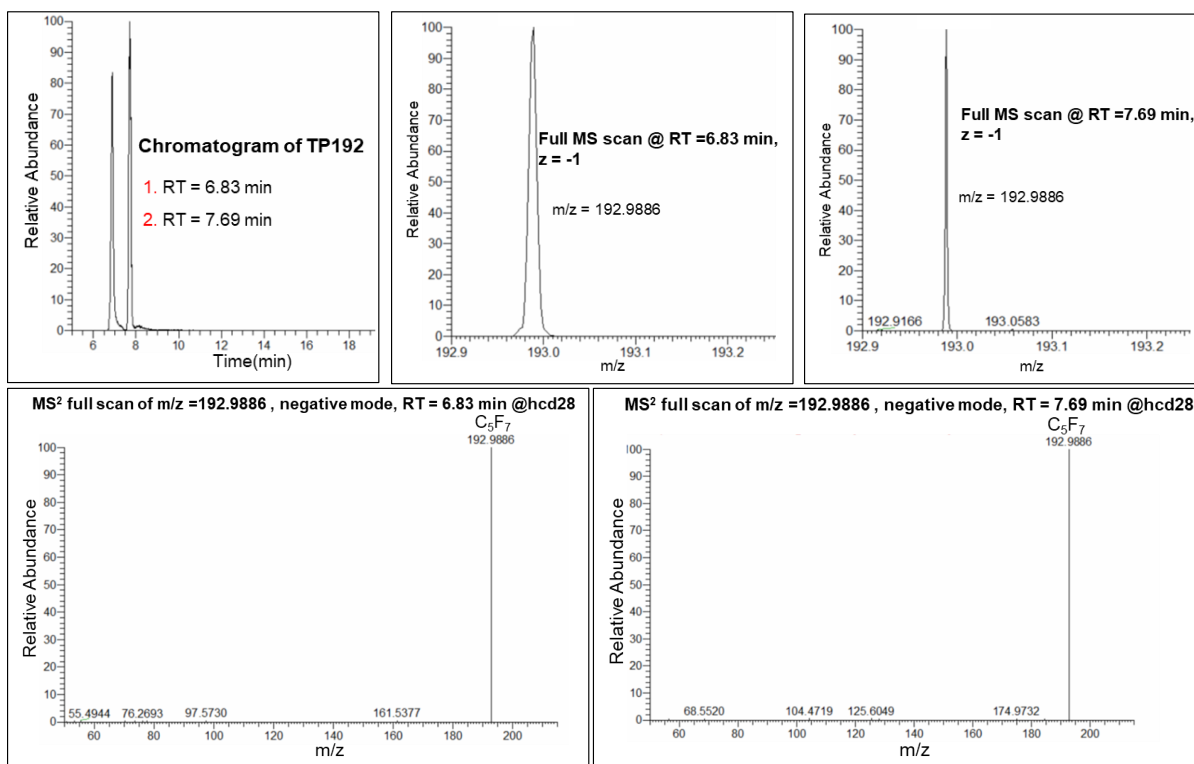
**Formula:** $C_6H_3F_7O_2$

**Atomic Modification:** −2F +2H of PFMeUPA

**Confirmed Structure:**
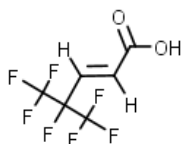


**Confidence level**: 1

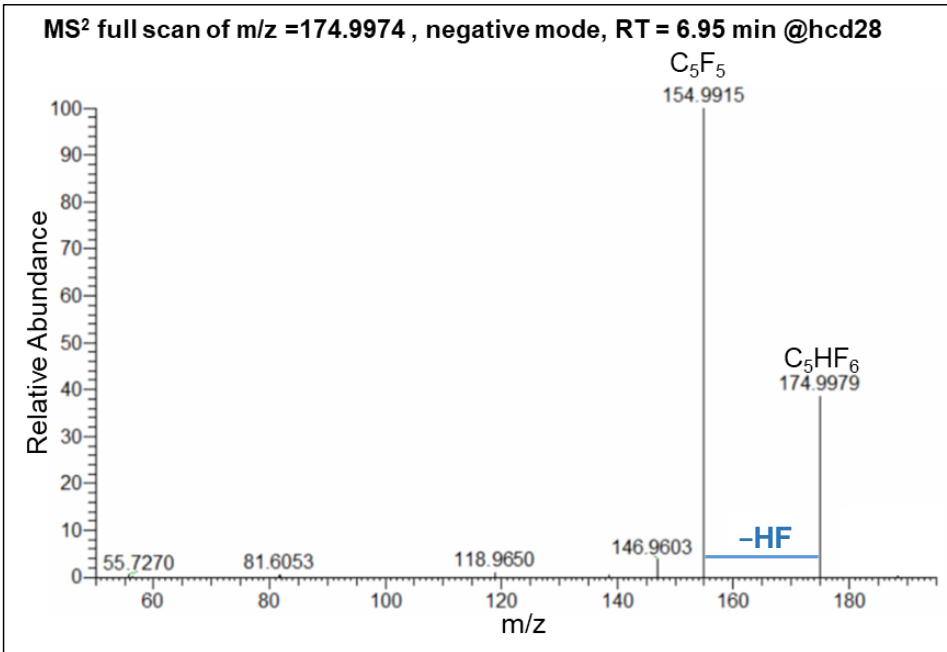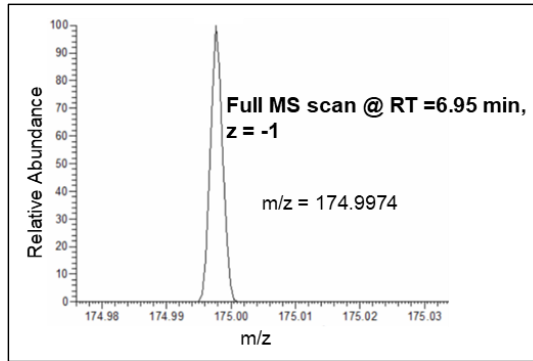**Fig. S13.** TP238 structure elucidation

**Formula:** $C_5HF_7$

**Atomic Modification:** $-CO_2 - 2F$ of PFMeUPA

**Confidence level**: 3

**Fig. S14.** TP192 structure elucidation

**Fig. S15.** TP174 structure elucidation
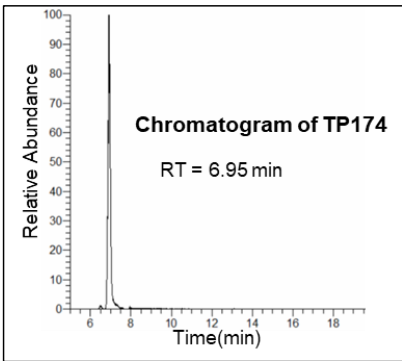
**Formula:** $C_5H_2F_6$

**Atomic Modification:** $-CO_2$ $-3F$ $+H$ of PFMeUPA
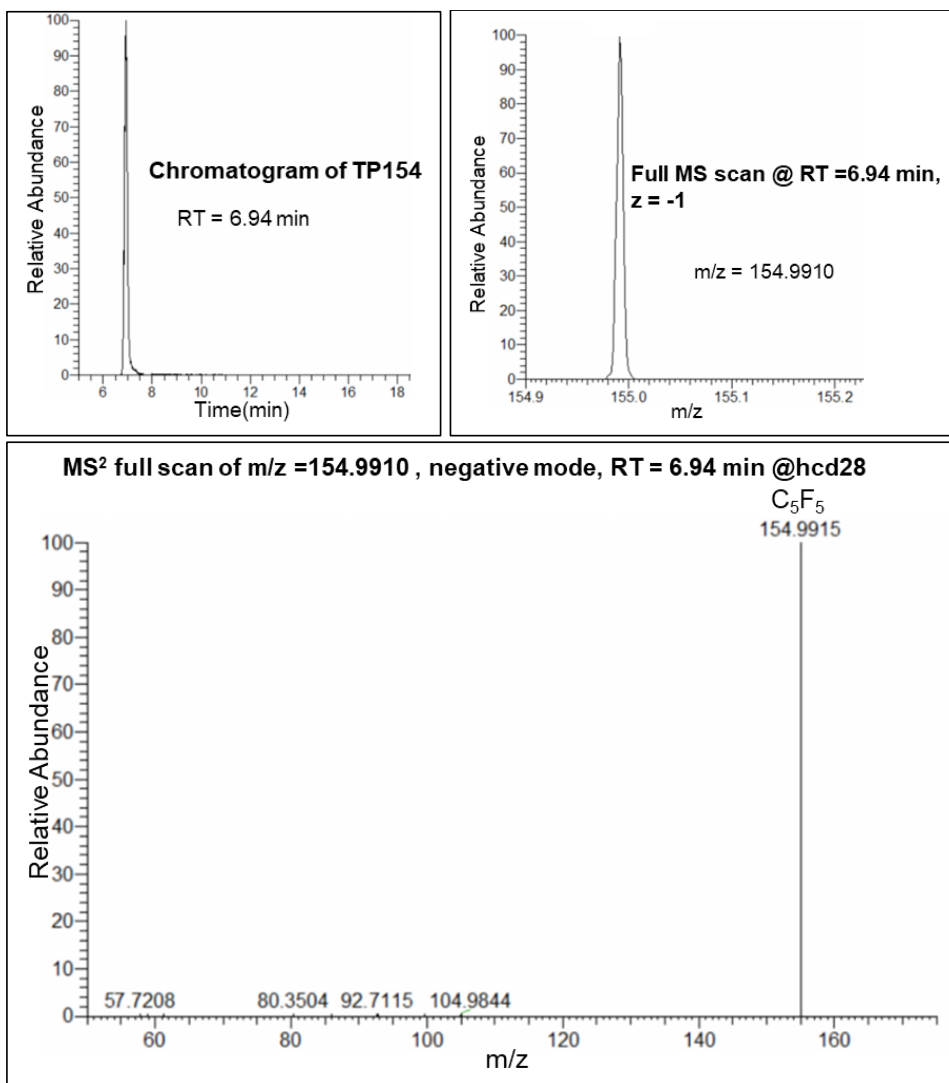
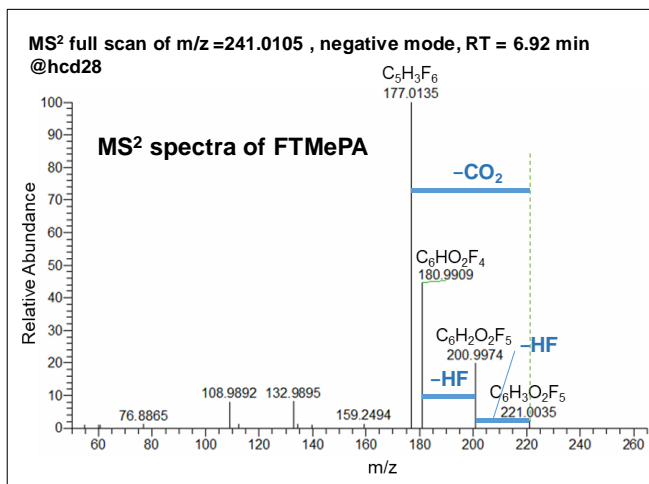**Confidence level**: 3

**Formula:** $C_5HF_5$

**Atomic Modification:** $-CO_2$ $-4F$ of PFMeUPA

**Confidence level**: 3

**Fig. S16.** TP154 structure elucidation
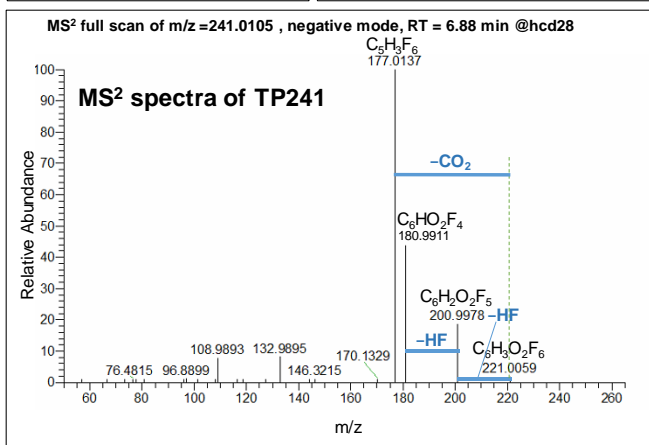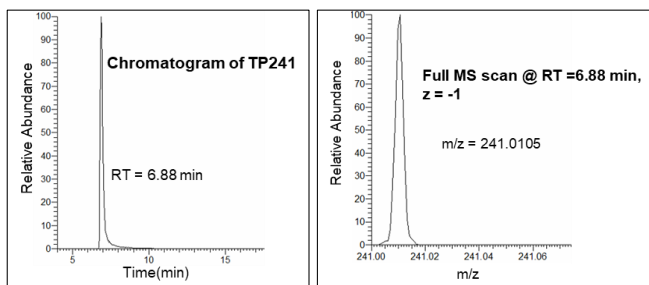
**Formula:** $C_6H_5F_7O_2$

**Atomic Modification:** +2H of FTMeUPA

**Confidence level**: 1

**Confirmed Structure:**
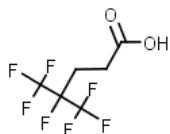


**Fig. S17.** TP241 structure elucidation
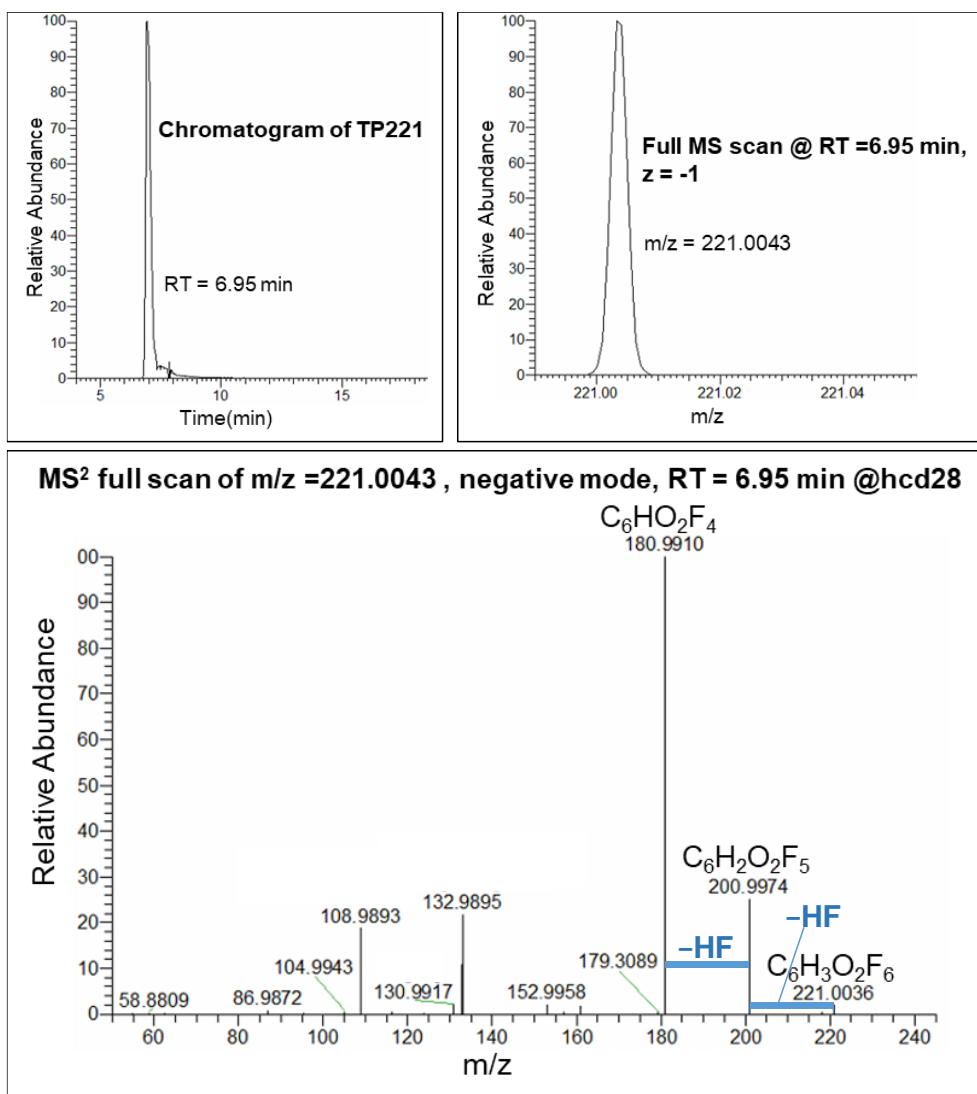
**Formula:** $C_6H_4F_6O_2$

**Atomic Modification:** −F +H of FTMeUPA

**Confidence level**: 2b

**Hypothetical Structure:**
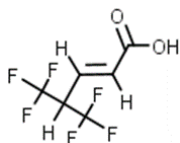


**Fig. S18.** TP221 structure elucidation

35
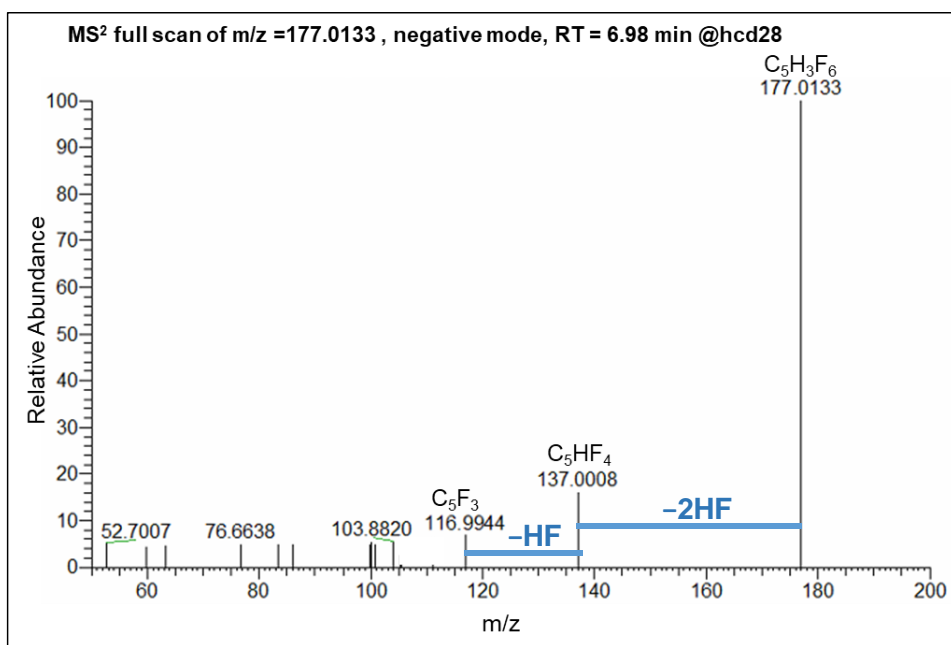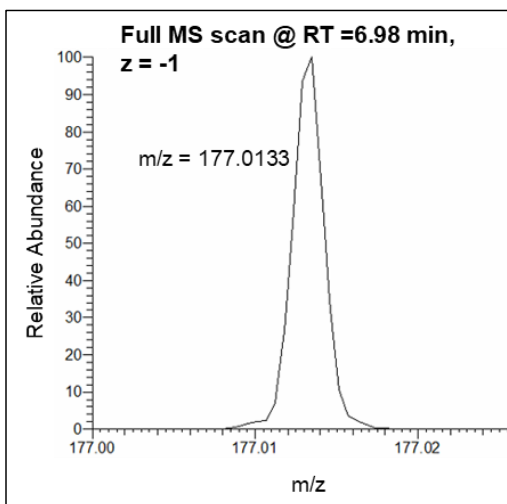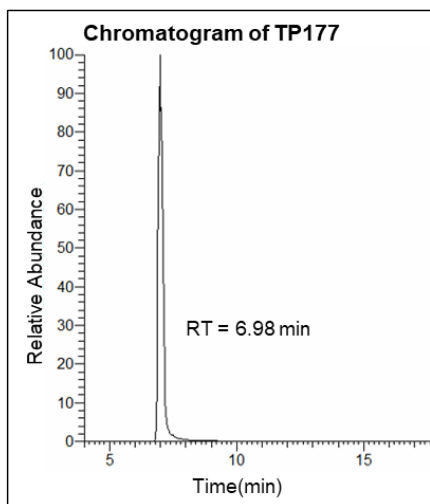
**Formula:** $C_5H_4F_6$

**Atomic Modification:** $-F$ $+H$ $-CO_2$ of FTMeUPA

**Confidence level**: 2b

**Hypothetical Structure:**
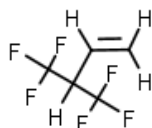


**Fig. S19.** TP177 structure elucidation
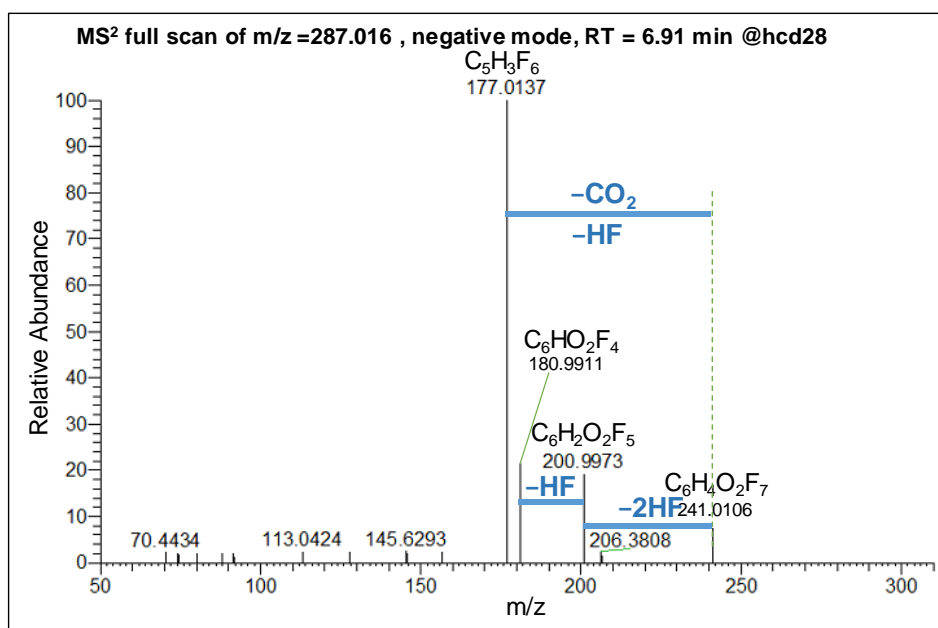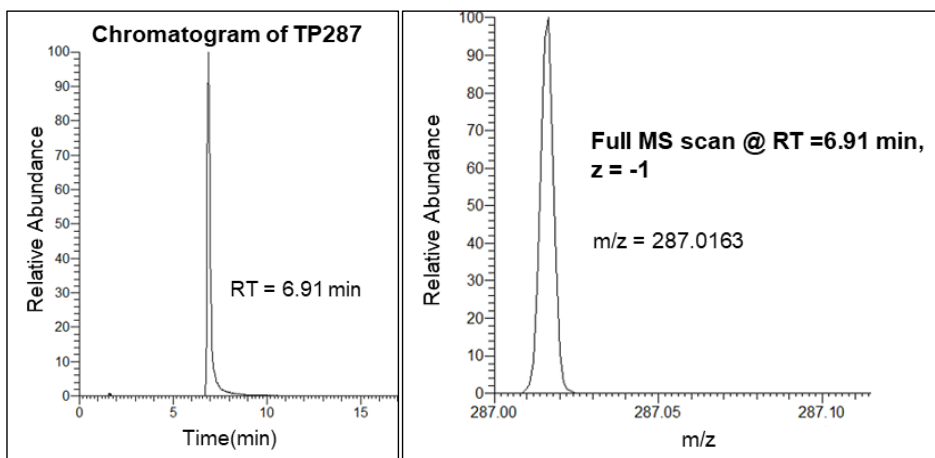
**Formula:** $C_7H_7F_7O_4$

**Atomic Modification:** +C +4H of FTMeUPA

**Confidence level**: 3

**Fig. S20.** TP287 structure elucidation
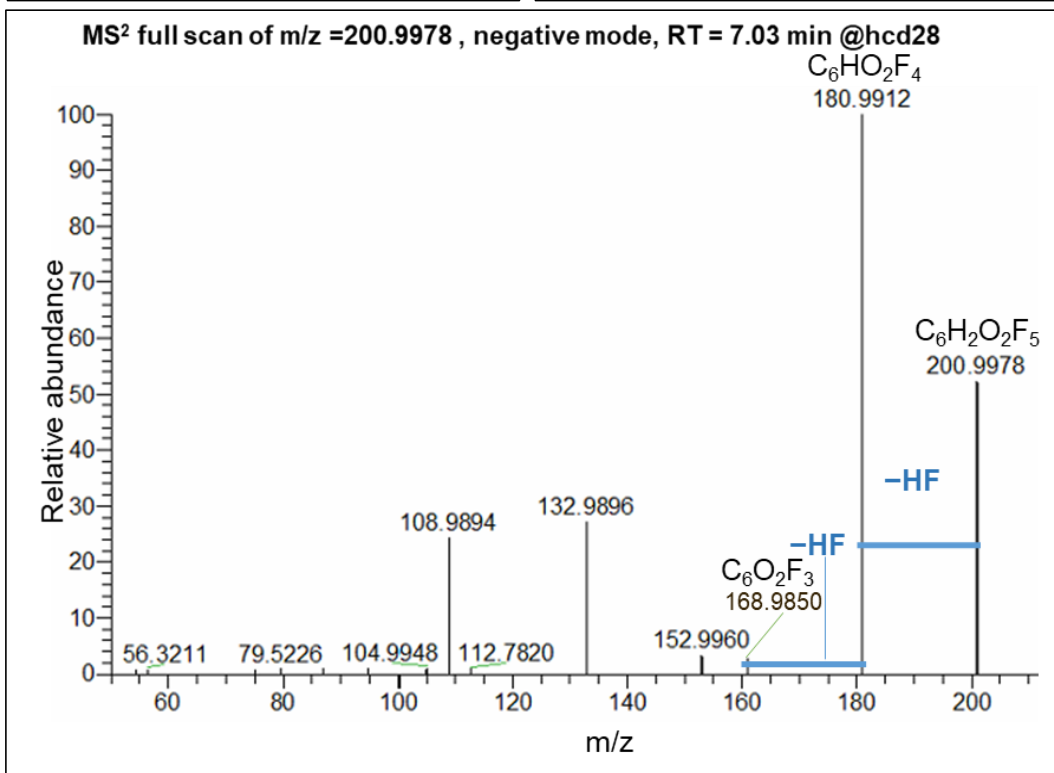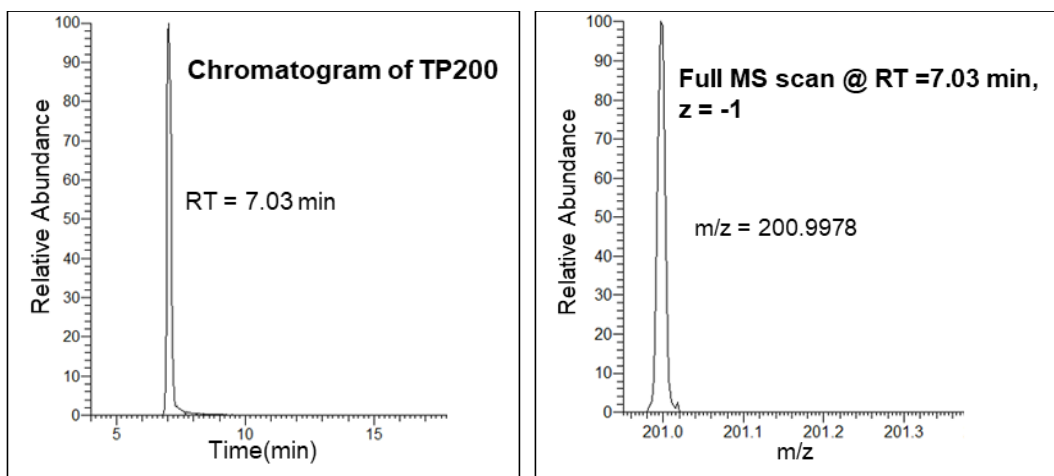
**Formula:** $C_6H_3F_5O_2$

**Atomic Modification:** −2F of FTMeUPA

**Confidence level**: 3

**Fig. S21.** TP200 structure elucidation
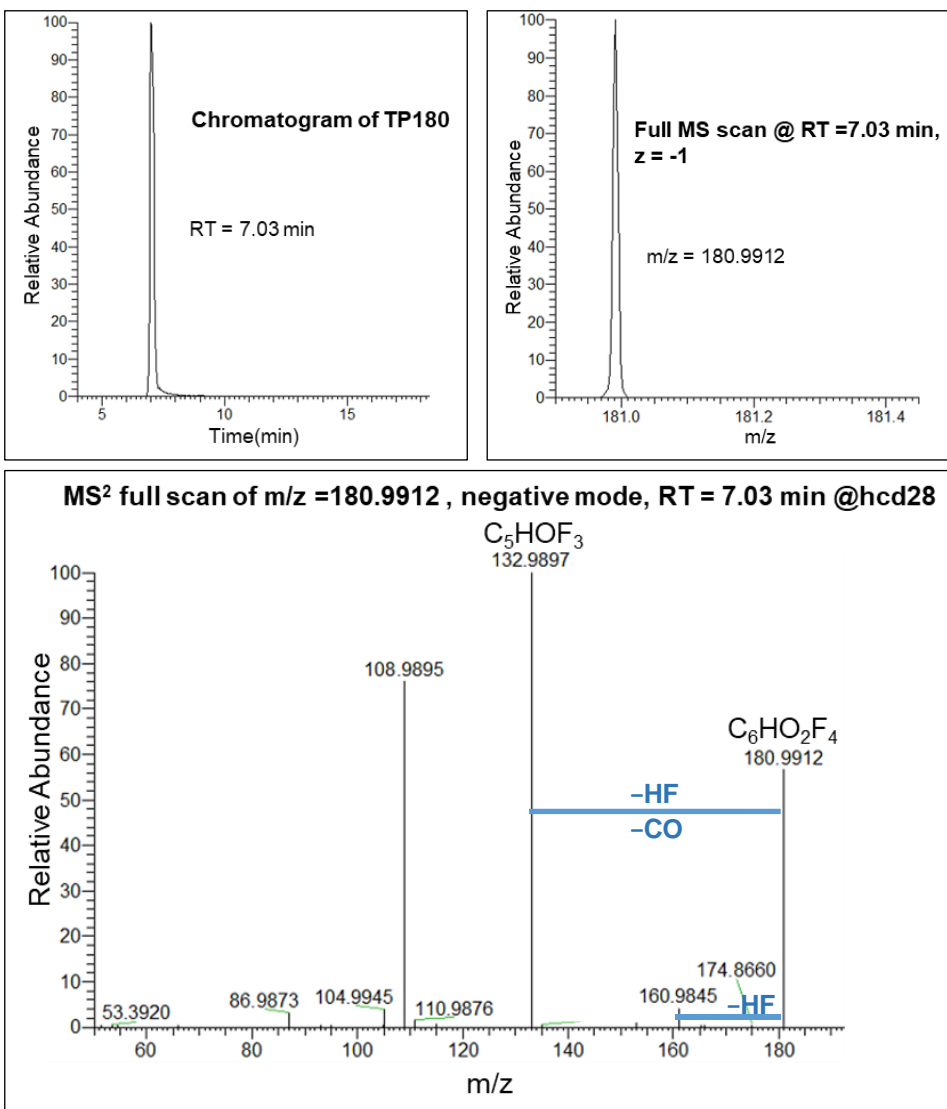
**Formula:** $C_6H_3F_5O_2$

**Atomic Modification:** −3F −H of FTMeUPA

**Confidence level**: 3

**Fig. S22.** TP180 structure elucidation
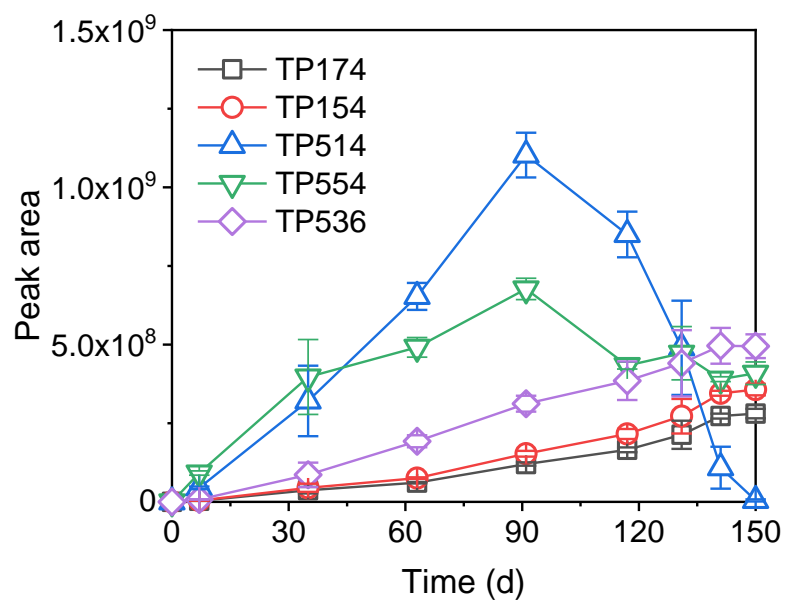
**Fig. S23.** Formation of minor PFMeUPA TPs.
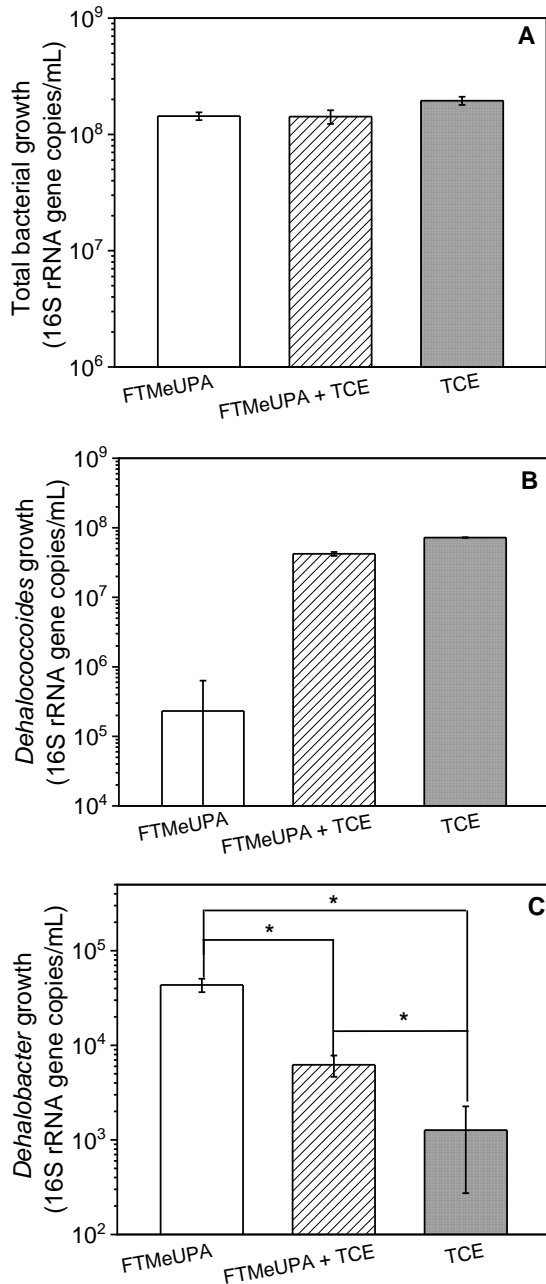
**Fig. S24.** Total bacterial growth (A), the growth of *Dehalococcoides* spp. (B), and *Dehalobacter* spp. (C) after 70 days in FTMeUPA defluorination experiments (* indicates significant difference between the two samples, $p < 0.05$, $n = 3$).
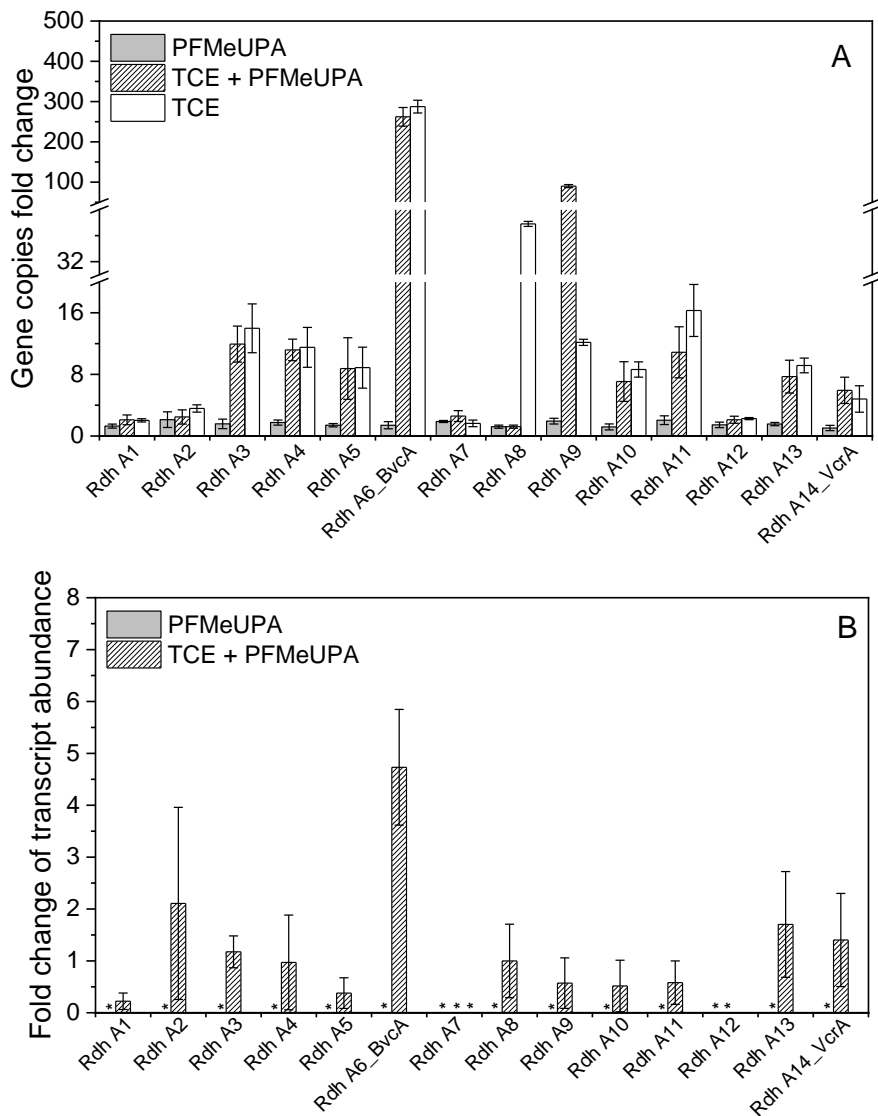
**Fig. S25.** Fold changes (91d/0d) of RDH gene copy numbers (A) and relative gene expression

levels (transcripts) of RDH genes in PFMeUPA-added samples in comparison to those in TCE-

added samples on 77d (B) (16S rRNA gene is the reference gene; n=3; *: no gene expression).
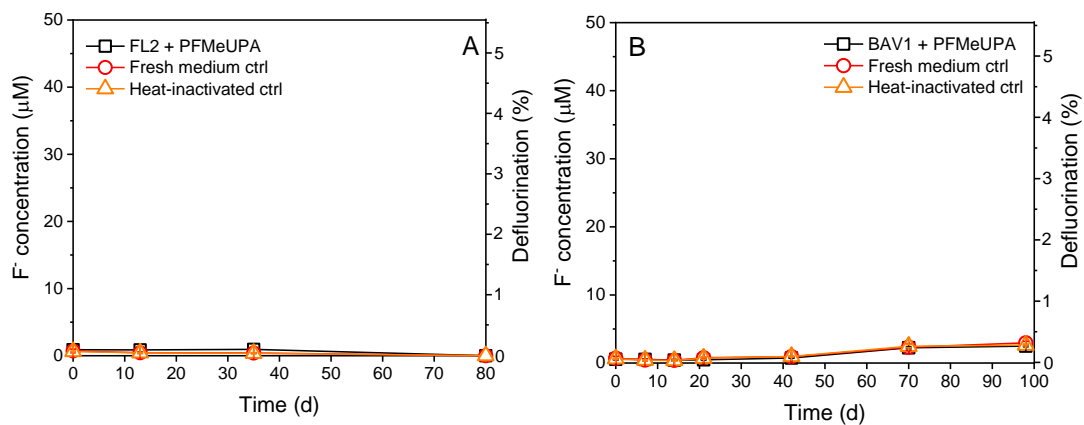
**Fig. S26.** Biotransformation of PFMeUPA by FL2 (A) and BAV1 (B).
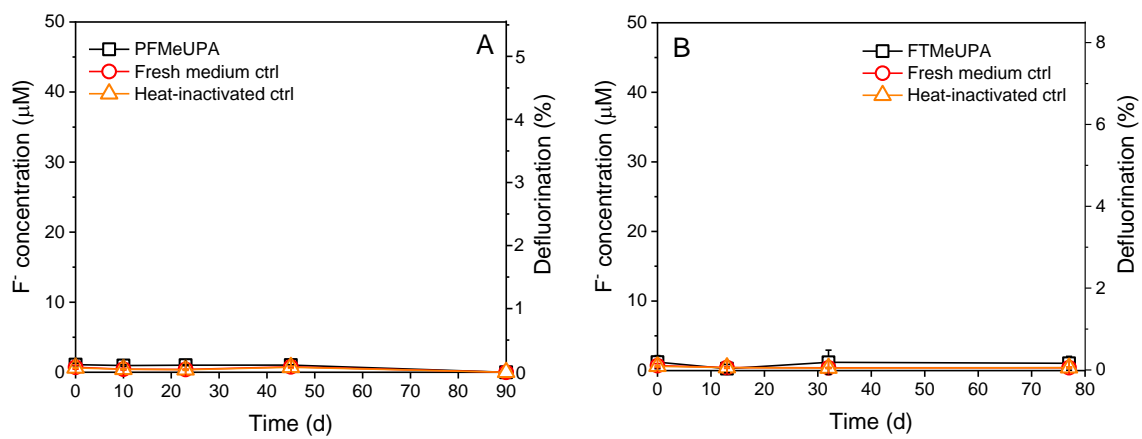
**Fig. S27.** Biotransformation of PFMeUPA (A) and FTMeUPA (B) by *Dehalobacter restrictus.*

**References**

(1) Wang, Z.; DeWitt, J. C.; Higgins, C. P.; Cousins, I. T. A never-ending story of per- and polyfluoroalkyl substances (PFASs)? *Environ. Sci. Technol.* **51**, 2508-2518 (2017).

(2) D'Agostino, L. A.; Mabury, S. A. Identification of novel fluorinated surfactants in aqueous film forming foams and commercial surfactant concentrates. *Environ. Sci. Technol.* **48**, 121-129 (2014).

(3) Xiao, F.; Golovko, S. A.; Golovko, M. Y. Identification of novel non-ionic, cationic, zwitterionic, and anionic polyfluoroalkyl substances using UPLC-TOF-MS(E) high-resolution parent ion search. *Anal. Chim. Acta.* **988**, 41-49 (2017).

(4) Xiao, F. Emerging poly- and perfluoroalkyl substances in the aquatic environment: a review of current literature. *Water Res.* **124**, 482-495 (2017).

(5) Sun, M.; Arevalo, E.; Strynar, M.; Lindstrom, A.; Richardson, M.; Kearns, B.; Pickett, A.; Smith, C.; Knappe, D. R. U. Legacy and emerging perfluoroalkyl substances are important drinking water contaminants in the Cape Fear River watershed of North Carolina. *Environ. Sci. Technol. Lett.* **3**, 415-419 (2016).

(6) Boulanger, B.; Vargo, J. D.; Schnoor, J. L.; Hornbuckle, K. C. Evaluation of perfluorooctane surfactants in a wastewater treatment system and in a commercial surface protection product. *Environ. Sci. Technol.* **39**, 5524-5530 (2005).

(7) Lindstrom, A. B.; Strynar, M. J.; Delinsky, A. D.; Nakayama, S. F.; McMillan, L.; Libelo, E. L.; Neill, M.; Thomas, L. Application of WWTP biosolids and resulting perfluorinated

compound contamination of surface and well water in Decatur, Alabama, USA. *Environ. Sci. Technol.* **45**, 8015-8021 (2011).

(8) Sepulvado, J. G.; Blaine, A. C.; Hundal, L. S.; Higgins, C. P. Occurrence and fate of perfluorochemicals in soil following the land application of municipal biosolids. *Environ. Sci. Technol.* **45**, 8106-8112 (2011).

(9) U.S. Environmental Protection Agency, (EPA). "PFOA & PFOS drinking water health advisories"; (Publication 800-F-16-003, EPA, 2016, www.epa.gov/sites/production/files/2016-06/documents/drinkingwaterhealthadvisories_pfoa_pfos_updated_5.31.16.pdf).

(10) Liu, J.; Van Hoomissen, D. J.; Liu, T.; Maizel, A.; Huo, X.; Fernández, S. R.; Ren, C.; Xiao, X.; Fang, Y.; Schaefer, C. E.; Higgins, C. P.; Vyas, S.; Strathmann, T. J. Reductive defluorination of branched per- and polyfluoroalkyl substances with cobalt complex catalysts. *Environ. Sci. Technol. Lett.* **5**, 289-294 (2018).

(11) Schaefer, C. E.; Choyke, S.; Ferguson, P. L.; Andaya, C.; Burant, A.; Maizel, A.; Strathmann, T. J.; Higgins, C. P. Electrochemical transformations of perfluoroalkyl acid (PFAA) precursors and PFAAs in groundwater impacted with aqueous film forming foams. *Environ. Sci. Technol.* **52**, 10689-10697 (2018).

(12) Vecitis, C. D.; Park, H.; Cheng, J.; Mader, B. T.; Hoffmann, M. R. Treatment technologies for aqueous perfluorooctanesulfonate (PFOS) and perfluorooctanoate (PFOA). *Front. Environ. Sci. Eng.* **3**, 129-151 (2009).

(13) Stratton, G. R.; Dai, F.; Bellona, C. L.; Holsen, T. M.; Dickenson, E. R. V.; Mededovic

Thagard, S. Plasma-based water treatment: Efficient transformation of perfluoroalkyl substances in prepared solutions and contaminated groundwater. *Environ. Sci. Technol.* **51**, 1643-1648 (2017).

(14) Bentel, M. J.; Yu, Y. C.; Xu, L. H.; Li, Z.; Wong, B. M.; Men, Y. J.; Liu, J. Y. Defluorination of per- and polyfluoroalkyl substances (PFASs) with hydrated electrons: structural dependence and implications to PFAS remediation and management. *Environ. Sci. Technol.* **53**, 3718-3728 (2019).

(15) Goldman, P. The enzymatic cleavage of the carbon-fluorine bond in fluoroacetate. *J. Biol. Chem.* **240**, 3434-3438 (1965).

(16) Visscher, P. T.; Culbertson, C. W.; Oremland, R. S. Degradation of trifluoroacetate in oxic and anoxic sediments. *Nature* **369**, 729-731 (1994).

(17) Kim, B. R.; Suidan, M. T.; Wallington, T. J.; Du, X. Biodegradability of trifluoroacetic acid. *Environ. Eng. Sci.* **17**, 337-342 (2000).

(18) Tiedt, O.; Mergelsberg, M.; Eisenreich, W.; Boll, M. Promiscuous defluorinating enoyl-CoA hydratases/hydrolases allow for complete anaerobic degradation of 2-fluorobenzoate. *Front. Microbiol.* **8**, 2579 (2017).

(19) Tiedt, O.; Mergelsberg, M.; Boll, K.; Muller, M.; Adrian, L.; Jehmlich, N.; von Bergen, M.; Boll, M. ATP-dependent C-F bond cleavage allows the complete degradation of 4-fluoroaromatics without oxygen. *Mbio* **7**, e00990-16 (2016).

(20) Wang, N.; Szostek, B.; Buck, R. C.; Folsom, P. W.; Sulecki, L. M.; Capka, V.; Berti, W. R.;

Gannon, J. T. Fluorotelomer alcohol biodegradation-direct evidence that perfluorinated carbon chains breakdown. *Environ. Sci. Technol.* **39**, 7516-7528 (2005).

(21) Shaw, D. M. J.; Munoz, G.; Bottos, E. M.; Duy, S. V.; Sauve, S.; Liu, J.; Van Hamme, J. D. Degradation and defluorination of 6:2 fluorotelomer sulfonamidoalkyl betaine and 6:2 fluorotelomer sulfonate by *Gordonia* sp. strain NB4-1Y under sulfur-limiting conditions. *Sci. Total. Environ.* **647**, 690-698 (2019).

(22) Zhang, S.; Szostek, B.; McCausland, P. K.; Wolstenholme, B. W.; Lu, X.; Wang, N.; Buck, R. C. 6:2 and 8:2 fluorotelomer alcohol anaerobic biotransformation in digester sludge from a WWTP under methanogenic conditions. *Environ. Sci. Technol.* **47**, 4227-4235 (2013).

(23) Lee, H.; D'eon, J.; Mabury, S. A. Biodegradation of polyfluoroalkyl phosphates as a source of perfluorinated acids to the environment. *Environ. Sci. Technol.* **44**, 3305-3310 (2010).

(24) Li, F.; Su, Q. F.; Zhou, Z. M.; Liao, X. B.; Zou, J.; Yuan, B. L.; Sun, W. J. Anaerobic biodegradation of 8:2 fluorotelomer alcohol in anaerobic activated sludge: metabolic products and pathways. *Chemosphere* **200**, 124-132 (2018).

(25) Butt, C. M.; Muir, D. C.; Mabury, S. A. Biotransformation pathways of fluorotelomer-based polyfluoroalkyl substances: a review. *Environ. Toxicol. Chem.* **33**, 243-267 (2014).

(26) Liu, J.; Mejia Avendano, S. Microbial degradation of polyfluoroalkyl chemicals in the environment: a review. *Environ. Int.* **61**, 98-114 (2013).

(27) Parsons, J. R.; Sáez, M.; Dolfing, J.; de Voogt, P. "Biodegradation of perfluorinated compounds" in *Reviews of environmental contamination and toxicology*, Whitacre, D. M., Ed.

(Springer US, 2008); vol. 196 pp. 53-71.

(28) Park, S.; de Perre, C.; Lee, L. S. Alternate reductants with $VB_{12}$ to transform C8 and C6 perfluoroalkyl sulfonates: limitations and insights into isomer specific transformation rates, products and pathways. *Environ. Sci. Technol.* **51**, 13869-13877 (2017).

(29) Fincker, M.; Spormann, A. M. Biochemistry of catabolic reductive dehalogenation. *Annu. Rev. Biochem.* **86**, 357-386 (2017).

(30) Schubert, T.; Adrian, L.; Sawers, R. G.; Diekert, G. Organohalide respiratory chains: composition, topology and key enzymes. *FEMS Microbiol. Ecol.* **94**, (2018).

(31) Ochoa-Herrera, V.; Field, J. A.; Luna-Velasco, A.; Sierra-Alvarez, R. Microbial toxicity and biodegradability of perfluorooctane sulfonate (PFOS) and shorter chain perfluoroalkyl and polyfluoroalkyl substances (PFASs). *Environ. Sci. Process. Impacts* **18**, 1236-1246 (2016).

(32) Pon, A.; Wishart, D.; Wilson, M.; Greiner, R.; Allen, F. CFM-ID: a web server for annotation, spectrum prediction and metabolite identification from tandem mass spectra. *Nucleic Acids Res.* **42**, W94-W99 (2014).

(33) Im, J.; Walshe-Langford, G. E.; Moon, J. W.; Löffler, F. E. Environmental fate of the next generation refrigerant 2,3,3,3-tetrafluoropropene (HFO-1234yf). *Environ. Sci. Technol.* **48**, 13181-13187 (2014).

(34) Tischer, W.; Bader, J.; Simon, H. Purification and some properties of a hitherto-unknown enzyme reducing the carbon-carbon double bond of α,β-unsaturated carboxylate anions. *Eur. J. Biochem.* **97**, 103-112 (1979).

(35) Winkler, C. K.; Tasnádi, G.; Clay, D.; Hall, M.; Faber, K. Asymmetric bioreduction of activated alkenes to industrially relevant optically active compounds. *J. Biotechnol.* **162**, 381-389 (2012).

(36) Dinglasan, M. J. A.; Ye, Y.; Edwards, E. A.; Mabury, S. A. Fluorotelomer alcohol biodegradation yields poly- and perfluorinated acids. *Environ. Sci. Technol.* **38**, 2857-2864 (2004).

(37) Duhamel, M.; Edwards, E. A. Microbial composition of chlorinated ethene-degrading cultures dominated by *Dehalococcoides*. *FEMS Microbiol. Ecol.* **58**, 538-549 (2006).

(38) Löffler, F. E.; Yan, J.; Ritalahti, K. M.; Adrian, L.; Edwards, E. A.; Konstantinidis, K. T.; Müller, J. A.; Fullerton, H.; Zinder, S. H.; Spormann, A. M. *Dehalococcoides mccartyi* gen. nov., sp. nov., obligately organohalide-respiring anaerobic bacteria relevant to halogen cycling and bioremediation, belong to a novel bacterial class, *Dehalococcoidia* classis nov., order *Dehalococcoidales* ord. nov. and family *Dehalococcoidaceae* fam. nov., within the phylum *Chloroflexi*. *Int. J. Syst. Evol. Microbiol.* **63**, 625-635 (2015).

(39) Waller, A. S.; Krajmalnik-Brown, R.; Löffler, F. E.; Edwards, E. A. Multiple reductive-dehalogenase-homologous genes are simultaneously transcribed during dechlorination by *Dehalococcoides*-containing cultures. *Appl. Environ. Microbiol.* **71**, 8257-8264 (2005).

(40) Puentes Jácome, L. A.; Edwards, E. A. A switch of chlorinated substrate causes emergence of a previously undetected native *Dehalobacter* population in an established *Dehalococcoides*-dominated chloroethene-dechlorinating enrichment culture. *FEMS Microbiol. Ecol.* **93**, fix141

(2017).

(41) Nelson, J. L.; Jiang, J.; Zinder, S. H. Dehalogenation of chlorobenzenes, dichlorotoluenes, and tetrachloroethene by three *Dehalobacter* spp. *Environ. Sci. Technol.* **48**, 3776-3782 (2014).

(42) Alfán-Guzmán, R.; Ertan, H.; Manefield, M.; Lee, M. Isolation and characterization of *Dehalobacter* sp. strain TeCB1 including identification of TcbA: a novel tetra- and trichlorobenzene reductive dehalogenase. *Front. Microbiol.* **8**, 558 (2017).

(43) Bao, Y. X.; Qu, Y. X.; Huang, J.; Cagnetta, G.; Yu, G.; Weber, R. First assessment on degradability of sodium *p*-perfluorous nonenoxybenzene sulfonate (OBS), a high volume alternative to perfluorooctane sulfonate in fire-fighting foams and oil production agents in China. *RSC Adv.* **7**, 46948-46957 (2017).

(44) Washington, J. W.; Jenkins, T. M.; Weber, E. J. Identification of unsaturated and 2H polyfluorocarboxylate homologous series and their detection in environmental samples and as polymer degradation products. *Environ. Sci. Technol.* **49**, 13256-13263 (2015).

(45) Men, Y. J.; Feil, H.; VerBerkmoes, N. C.; Shah, M. B.; Johnson, D. R.; Lee, P. K. H.; West, K. A.; Zinder, S. H.; Andersen, G. L.; Alvarez-Cohen, L. Sustainable syntrophic growth of *Dehalococcoides ethenogenes* strain 195 with *Desulfovibrio vulgaris Hildenborough* and *Methanobacterium congolense*: global transcriptomic and proteomic analyses. *ISME J.* **6**, 410-421 (2012).

(46) He, J.; Holmes, V. F.; Lee, P. K.; Alvarez-Cohen, L. Influence of vitamin $B_{12}$ and cocultures on the growth of *Dehalococcoides* isolates in defined medium. *Appl. Environ. Microbiol.* **73**,

2847-2853 (2007).

(47) Yu, Y. C.; Han, P.; Zhou, L. J.; Li, Z.; Wagner, M.; Men, Y. J. Ammonia monooxygenase-mediated cometabolic biotransformation and hydroxylamine-mediated abiotic transformation of micropollutants in an AOB/NOB coculture. *Environ. Sci. Technol.* **52**, 9196-9205 (2018).

(48) Zhou, L. J.; Han, P.; Yu, Y.; Wang, B.; Men, Y.; Wagner, M.; Wu, Q. L. Cometabolic biotransformation and microbial-mediated abiotic transformation of sulfonamides by three ammonia oxidizers. *Water Res.* **159**, 444-453 (2019).

(49) Men, Y.; Han, P.; Helbling, D. E.; Jehmlich, N.; Herbold, C.; Gulde, R.; Onnis-Hayden, A.; Gu, A. Z.; Johnson, D. R.; Wagner, M.; Fenner, K. Biotransformation of two pharmaceuticals by the ammonia-oxidizing archaeon *Nitrososphaera gargensis*. *Environ. Sci. Technol.* **50**, 4682-4692 (2016).

(50) Becke, A. D. Density-functional thermochemistry. III. The role of exact exchange. *J. Chem. Phys.* **98**, 5648-5652 (1993).

(51) Lee, C.; Yang, W.; Parr, R. G. Development of the Colle-Salvetti correlation-energy formula into a functional of the electron density. *Phys. Rev. B* **37**, 785-789 (1988).

(52) Stephens, P.; Devlin, F.; Chabalowski, C.; Frisch, M. J. Ab initio calculation of vibrational absorption and circular dichroism spectra using density functional force fields. *J. Phys. Chem.* **98**, 11623-11627 (1994).

(53) Vosko, S. H.; Wilk, L.; Nusair, M. Accurate spin-dependent electron liquid correlation energies for local spin density calculations: a critical analysis. *Can. J. Phys.* **58**, 1200-1211

(1980).

(54) Grimme, S.; Ehrlich, S.; Goerigk, L. Effect of the damping function in dispersion corrected density functional theory. *J. Comput. Chem.* **32**, 1456-1465 (2011).

(55) Marenich, A. V.; Cramer, C. J.; Truhlar, D. G. Universal solvation model based on solute electron density and on a continuum model of the solvent defined by the bulk dielectric constant and atomic surface tensions. *J. Phys. Chem. B* **113**, 6378-6396 (2009).

(56) Livak, K. J.; Schmittgen, T. D. Analysis of relative gene expression data using real-time quantitative PCR and the $2^{-\Delta\Delta CT}$ method. *Methods* **25**, 402-408 (2001).

(57) Mei, R.; Narihiro, T.; Nobu, M. K.; Kuroda, K.; Liu, W. T. Evaluating digestion efficiency in full-scale anaerobic digesters by identifying active microbial populations through the lens of microbial activity. *Sci Rep.* **6**, 34090 (2016).

(58) Sonthiphand, P.; Neufeld, J. D. Evaluating primers for profiling anaerobic ammonia oxidizing bacteria within freshwater environments. *PLoS One* **8**, e57242 (2013).

(59) Seshadri, R.; Adrian, L.; Fouts, D. E.; Eisen, J. A.; Phillippy, A. M.; Methe, B. A.; Ward, N. L.; Nelson, W. C.; Deboy, R. T.; Khouri, H. M.; Kolonay, J. F.; Dodson, R. J.; Daugherty, S. C.; Brinkac, L. M.; Sullivan, S. A.; Madupu, R.; Nelson, K. T.; Kang, K. H.; Impraim, M.; Tran, K.; Robinson, J. M.; Forberger, H. A.; Fraser, C. M.; Zinder, S. H.; Heidelberg, J. F. Genome sequence of the PCE-dechlorinating bacterium *Dehalococcoides ethenogenes*. *Science* **307**, 105-108 (2005).

(60) MaymoGatell, X.; Chien, Y. T.; Gossett, J. M.; Zinder, S. H. Isolation of a bacterium that

reductively dechlorinates tetrachloroethene to ethene. *Science* **276**, 1568-1571 (1997).

(61) Holmes, V. F.; He, J. Z.; Lee, P. K. H.; Alvarez-Cohen, L. Discrimination of multiple

*Dehalococcoides* strains in a trichloroethene enrichment by quantification of their reductive

dehalogenase genes. *Appl. Environ. Microbiol.* **72**, 5877-5883 (2006).

(62) Grostern, A.; Edwards, E. A. Characterization of a *Dehalobacter* coculture that dechlorinates

1,2-dichloroethane to ethene and identification of the putative reductive dehalogenase gene.

*Appl. Environ. Microbiol.* **75**, 2684-2693 (2009).